Inhibition of the Nonessential Neurovirulence Gene of Herpes Simplex Virus Type 1 Using RNA Interference

Master's Thesis

University of Turku

MSc Degree Programme in Biomedical Sciences

Drug Discovery and Development

4/2021

Fanny Frejborg

Supervised by Veijo Hukkanen and Marie Nyman

Institute of Biomedicine, Infections and Immunity/Virology

The originality of this thesis has been verified in accordance with the University of Turku quality assurance system using the Turnitin Originality Check service

UNIVERSITY OF TURKU
Institute of Biomedicine, Faculty of Medicine

FREJBORG, FANNY: Inhibition of the nonessential neurovirulence gene of herpes simplex virus type 1 using RNA interference
Master's Thesis, 54 p
MSc Degree Programme in Biomedical Sciences, Drug Discovery and Development
April 2021

Herpes simplex virus type 1 (HSV-1) is a common pathogen that causes recurrent and latent infections in humans. The nonessential neurovirulence gene $\gamma_1$34.5 prevents cellular responses to an infection in differentiated host cells. The deletion of this gene makes HSV-1 conditionally replicative. Thereby most of the HSV-1 vectors and oncolytic viruses carry this deletion. The objective of this study was to assess whether targeting $\gamma_1$34.5 using RNA interference would be antiviral or gene-specific. The effects of six siRNAs targeting $\gamma_1$34.5 were studied *in vitro*. The cellular viability, antiviral efficacy, $\gamma_1$34.5 gene expression, and host responses were assessed. Three cell lines were used – U373MG representing neuronal cells, HCE representing epithelial cells, and Vero cells (non-human primate kidney). The viruses used were the recombinant wild type-like HSV-1(17+)LoxP$_{mCMV}$GFP and the HSV vector backbone H1052. The $\gamma_1$34.5 siRNAs were well tolerated in U373MG and HCE cells. The $\gamma_1$34.5 gene expression of the wild type–like virus was inhibited in U373MG cells. Some $\gamma_1$34.5 siRNA treatments induced a reduction in viral shedding whilst others an increase. This was correlated with the innate immunity, where the samples with an increase in viral shedding had a reduction in cellular responses. The successful inhibition of $\gamma_1$34.5 in U373MG cells shown in this study could be further developed into a new method for vector production and selection *in vitro*, or to new *in vivo* infection models with protection from severe infections, when using wild type-like viruses.

Keywords: Herpes Simplex, RNA interference, $\gamma_1$34.5, neurovirulence, viral vectors

Contents

1. Introduction

Herpes simplex viruses (HSV), viruses of the family *herpesviridae*, were the first human herpes viruses to be discovered and are among the most investigated (Knipe et al., 2013). Two species of HSV are recognized, HSV-1 and HSV-2. Both virus species cause latent and recurrent infections in humans and certain animal models, and when activated they most commonly cause oral or genital lesions, although HSV-1 more commonly in the orofacial region and HSV-2 in the genital region (Hukkanen and Seppänen, 2020). HSVs have a seroprevalence of around 80% worldwide, with a larger prevalence in the developing countries (Denes et al., 2020).

HSV transmits via close contact and is the most infectious when lesions are present (Hukkanen et al., 2020). HSV may develop latency in neuronal nuclei, mostly in the trigeminal nerve, and causes lytic infection in epithelial cells, mostly in the orofacial region, which is its primary infection site (Denes et al., 2020). HSV may reactivate from latency in, for example, the events of common colds, ultraviolet light, immune deficiency, hormonal changes, and stress, although the mechanism is not yet fully understood (Knipe et al., 2013).

1.1. HSV as a pathogen

1.1.1. Disease manifestations of HSV

Primary infections of HSV-1 are often subclinical and asymptomatic, and most commonly transmitted orally (Hukkanen and Seppänen, 2020). However, primary infections cause gingivostomatitis in 1-10% of cases, and are most prevalent in children aged 2-3, according to Hukkanen and Seppänen. Gingivistomatitis causes painful blisters, usually in the orofacial region, and may cause a fever.

Once latent, the infection is mostly asymptomatic (Hukkanen and Seppänen, 2020). HSV infections turn symptomatic during the reactivation of the virus, although in certain cases it remains asymptomatic. How often HSV reactivates varies greatly. HSV causes blisters and lesions at its transmission site, the orofacial or genital area.

Sometimes, HSV infection can induce erythema multiforme, which manifests on the skin or the mucous membrane. Erythema multiforme lesions are autoimmune reactions to HSV (Hukkanen and Seppänen, 2020). Other skin manifestations of HSV-1 include eczema herpeticum, which occurs in primary infections and can resemble shingles.

Rarely, HSV can cause herpes keratitis, an infection of the eye's cornea, which untreated can lead to blindness (Farooq and Shukla, 2012).

Another rare and severe manifestation of HSV is neonatal herpes, in which the mother infects the child during childbirth. The complication is most severe when the mother has a primary infection, and thus cannot provide the child with neutralizing antibodies (Brown et al., 2003). The most severe HSV infection is herpes encephalitis, which is life-threatening, with necrosis commonly seen in the frontal lobe (Kumar et al., 2013). The incidence is 1 in 200 000 per year, and manifests throughout every age group (Hukkanen and Seppänen, 2020). The information suggests that about a third of the cases are caused by primary infections. The mortality rate of encephalitis is 20%, however it commonly causes permanent, neurological complications. The prognosis of HSV encephalitis is better if treatment is started early, within 4 days of manifestation (Lumio, 2020). Untreated, the mortality rate is 70%, and of surviving patients only 2.5% regain normal neurological function (Knipe et al., 2013).

1.1.2. Treatment of HSV infections

The first-line treatment of both primary and recurrent infections of HSV is acyclovir, a nucleoside analogue which the viral protein thymidine kinase phosphorylates, terminating DNA replication in infected cells (Denes et al., 2020). According to Knipe et al. (2013), acyclovir shows high efficacy even in severe disease manifestations, both primary and recurrent forms of infection, and is well tolerated and safe, as the nucleoside analogue only interferes with infected cells. In severe recurrent infections, common in immunocompromised patients, acyclovir can also be used to prevent reactivation of the virus. Prophylactic therapy does reduce the frequency of recurrences, but viral shedding still occurs, making transmission of the virus possible. Valacyclovir, acyclovir's prodrug, and famciclovir, prodrug of penciclovir, have a similar mode of action, but a higher oral bioavailability. In immunosuppressed patients, prophylactic therapy leads to a progressive disease, suggesting the emergence of resistant strains, according to Knipe et al (2013). The most common mutation that leads to acyclovir resistance is a mutation of thymidine kinase.

There is no vaccine available for HSV, and the development of one is a high priority, as it would be the most ideal solution for the prevention of severe disease manifestations (Knipe et al., 2013). However, there are many challenges present for the development of

a vaccine, including HSV's ability to evade the host immune system, as well as the host's pre-existing humoral responses, according to the authors.

1.2. Biology of HSV

1.2.1. Virion structure

The HSV genome consists of double stranded DNA and is contained in an icosahedral capsid surrounded by an envelope. The tegument, which contains many of the virion's proteins, surrounds the icosahedral capsid. The envelope is the outermost layer and is a spiked bilayer consisting of lipids. The virion has an average diameter of 186 nm (Grünwald et al., 2003). The genome, icosahedral capsid, tegument and spiked bilayer are illustrated in **Figure 1**.

The viral DNA is linear and contains around 150 kilobase pairs (Knipe et al., 2013). The whole genome consists of two covalently bonded components, L and S, which can exist inverted relative to each other. The icosahedral capsid containing the DNA consists of an intermediate and an outer layer.

The tegument space that is situated between the capsid and the envelope is unstructured and 18 viral proteins have been discovered comprising the tegument (Loret et al., 2008). The virion transactivator protein, α-TIF (VP16), is an important viral protein that is contained in the tegument.

The envelope is a lipid bilayer with 13 viral glycoproteins on the surface (Knipe et al., 2013). The lipids are assumed to be acquired from the host.

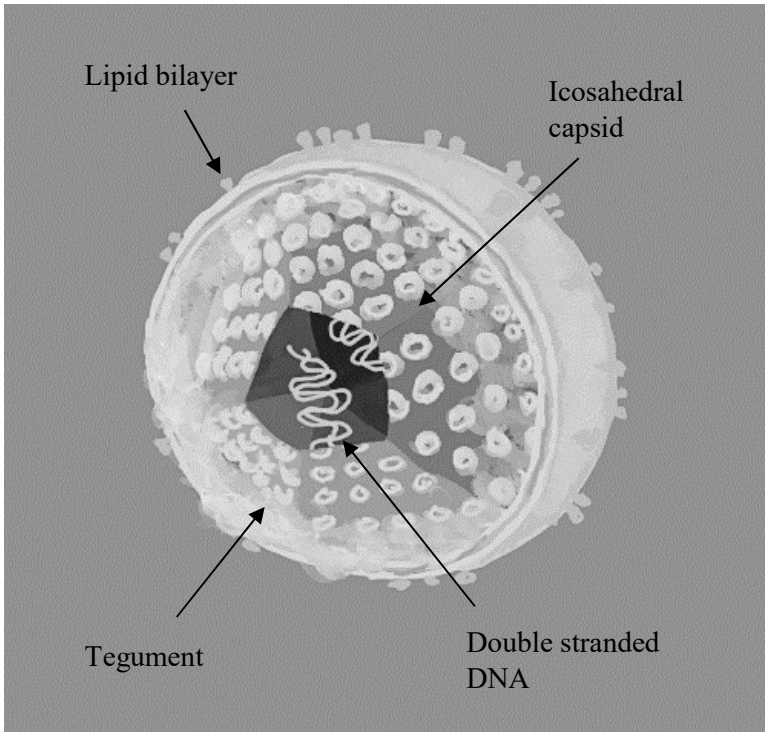

Figure 1. The structure of the HSV-1 virion. The genome of HSV-1 is contained in an icosahedral capsid, which is surrounded by the tegument. The tegumented capsid is contained in a spiked bilayer.

1.2.2. Attachment and entry to the host cell

The virus enters the cell by attaching to cell surface receptors with viral glycoproteins found on the envelope, after which the envelope fuses with the cell membrane and releases the tegumented capsid containing the DNA (Knipe et al., 2013).

There are at least five surface glycoproteins involved in the attachment and fusion of the virus to the cell (Knipe et al., 2013). The viral glycoproteins gB and gC bind to glycosaminoglycans on the cell, and this is followed by gD binding to nectin, herpesvirus entry mediator or 3-O-sulfated heparan sulfate (Connolly et al., 2011). However, the roles of the three cellular receptors are unclear. Furthermore, the roles of the viral glycoproteins gH and gL are also unknown. Knipe et al. believe that the binding to either of these receptors changes the conformation of gD, and subsequently activates gB, which is believed to lead to the fusion of the envelope with the cellular membrane.

Evidence shows that viral entry in Vero cells increases the levels intracellular calcium in the cell, and inhibiting this response prevents viral entry (Knipe et al., 2013). Thus, calcium signaling might be important for viral entry, according to Knipe et al. Once the envelope has fused with the cellular membrane, the capsid and tegument is released into the cytoplasm.

1.2.3. Replication, capsid assembly and egress

The tegumented capsid is transported to the nuclear pores where the DNA is released from the capsid through a pressure driven ejection mechanism (Sodeik et al., 1997). The DNA does not integrate into the cellular genome (Hukkanen and Seppänen, 2020). The transcription and replication of the viral DNA as well as the assembly of new viral capsids take place in the nucleus (Honess and Roizman., 1974; Mettenleiter, 2002). Host RNA polymerase II transcribes the viral DNA, with the participation of viral proteins. The viral gene expression takes place in the cytoplasm and is carefully regulated in a cascade manner, and the viral genes are classified according to their order in the gene expression cascade: α, β and γ (Honess and Roizman., 1974). The α genes do not require prior viral gene expression, β genes require at least two α genes to be expressed, and γ genes that in addition to α gene expression require viral DNA synthesis (Knipe et al., 2013). Examples of β genes are U_L29, which encodes infected cell protein (ICP) 8, a major viral DNA-binding protein that is essential for viral DNA synthesis, and U_L23, which encodes thymidine kinase (Knipe et al., 2013). The γ genes are largely involved in assembly of the new virion. Some of the viral proteins that are involved in viral DNA transcription are α-TIF, which derepresses α gene promoters and also activates the transcription by recruiting transcription factors, ICP4, which recruits transcriptional complexes involved in the transcription of post-α genes, and ICP0, which inactivates repressor complexes in non-neuronal cells and recruits several other factors (Knipe et al., 2013). The virus requires the host synthesis apparatus for translation, thus the virus inhibits host protein transcription and RNA splicing.

For the production of new virions, new viral DNA must be synthesized. Directly involved in this process are β gene products. For this process to initiate, viral DNA replication proteins migrate to the nuclear periphery and form prereplicative sites, and grow into replication compartments as the process proceeds (Liptak et al., 1996). The mechanism of the synthesis is not fully understood, but it is thought to be a two-stage. The first stage involves binding of viral U_L9 origin binding protein to the replication complex (Knipe et al. 2013). This stage yields circular progeny DNA. The second stage is thought to be either a rolling circle or recombinational mechanism, or a combination of both according to Knipe et al. Some of the proteins involved in the replication are the HSV DNA polymerase, which has a larger range of interaction with deoxynucleoside triphosphate than cellular polymerases, origin binding protein U_L9, the binding of which to the origin sequences induces a bend in the DNA, U_L29 gene product ICP8, which binds to single

stranded DNA and also interacts with other replication proteins, and DNA helicase-primase complex, which unwinds short oligonucleotides and synthesizes primers (Knipe et al., 2013).

For resting cells, the virus utilizes its gene products such as thymidine kinase, deoxyuridine triphosphatase, ribonucleotide reductase, and uracil DNA glycolase (Knipe et al., 2013). These are not essential for viral replication in active cells, but are needed for DNA synthesis in resting cells, such as neuronal cells.

The γ gene products migrate into the nucleus where they initiate the capsid assembly (Knipe et al., 2013). According to the literature, the capsid with internal scaffolding is first assembled and then the viral DNA is encapsidated, resulting in loss of the scaffolding. These capsids are about 150 nm in diameter. The egress of the capsid and formation of a mature virion is not yet understood, and three possible models exist, the dual envelopment model, the luminal pathway, and the nuclear pore egress pathway, as explained by Knipe et al. According to them, the dual envelopment model is favored currently; it involves the capsid budding from the inner nuclear envelope, where the capsid is bound to tegument proteins, followed by fusion of the envelope with the outer nuclear membrane, releasing the tegumented capsid into the cytoplasm. The tegumented capsid is then re-enveloped in perhaps the golgi apparatus membrane, and the enveloped tegumented capsid is then transported to the cellular membrane where it undergoes exocytosis. The luminal pathway is similar to that of the dual envelopment model, but instead of the capsid fusing with the nuclear membrane, it is contained in a perinuclear vesicle that fuses with the membrane and releases the enveloped tegumented capsid into the cytoplasm. The third model, the nuclear pore egress pathway, involves the capsid exiting the nucleus through pores, where it is enveloped in cytoplasmic membranes.

1.2.4. Latency

HSV's ability to form latency in neuronal cells is one of its most complex characteristics. Not only does this ability help the virus spread from older generations to younger generations, but also makes a cure or vaccine difficult to develop (Knipe et al., 2013).

At the site of the primary infection, the virus enters sensory nerves, and the tegumented capsid travels through retrograde axonal transport to sensory ganglia (Perng and Jones, 2010). Lytic infection is repressed and no replicating virus is present. High amounts of LAT genes are expressed, although no proteins encoded by LATs have been found (Stevens et al., 1987; Knipe et al., 2013). The function of LAT is not well understood -

however, it seems to suppress viral gene expression and replication, and the inhibition of LAT leads to higher replication in trigeminal tissue, as suggested by Knipe et al. The DNA in latently infected cells is circular or endless, assembled in nucleosomal chromatin. Periodical reactivations are poorly understood, however, a decrease in LAT level and lytic transcription initiation are detected. The viral genes are expressed in two waves: first there is a widespread burst of transcription of all lytic HSV genes, followed by an ordered cascade of gene expression leading to production of virus particles (Kim et al., 2012). Reactivation only produces a few virions in the neuronal ganglia, which travel through anterograde axonal transport typically to the site of the primary infection. Whether the neurons undergo lysis due to the reactivation is unknown. Reactivation has been achieved in animal models through ultraviolet light exposure, hyperthermia, peripheral tissue damage, and prostaglandin synthesis (Knipe et al., 2013).

1.2.5. Pathophysiology

For an infection to transmit, close contact between an HSV excreting person and a seronegative person must occur either through mucosal tissue or damaged skin (Knipe et al., 2013). HSV-1's primary infection site is usually the oropharyngeal area, and following primary infection the virus forms latency in the trigeminal ganglia. Latency is fundamental for recurrent HSV pathogenesis, and is the most dominant factor contributing to disease manifestation.

The changes seen in the infected tissue include virus-mediated cell death and inflammation (Knipe et al., 2013). The cells undergo ballooning and chromatin condenses and marginalizes within the nuclei of the cells (Myllys et al., 2016). The nuclei degenerate and the cells lose intact plasma membranes and form giant cells (Knipe et al., 2013). According to the authors, vesicular fluid containing cell debris, inflammatory cells, and multinucleated giant cells appears between the epidermis and dermis, associated with cell lysis. In mucous membranes, the vesicles rupture and form ulcers. Once healing occurs, the fluid becomes pustular and scabs, but uncommonly scars. In organs affected other than skin, prominent vascular changes can be observed, such as perivascular cuffing and hemorrhagic necrosis. In encephalitis, oligodendrocytic involvement, astrocytosis, and gliosis can be observed (Knipe et al., 2013; Meyding-Alamé et al. 1998).

1.2.6. Immune responses to HSV

The host defends itself from an HSV infection through a myriad of responses, such as innate immunity responses, specific antibodies, cytokine responses, natural killer cell responses, and local control mechanisms that can be either universal or HSV specific.

The initial response to an HSV infection is a secretion of type I interferons (IFN) (Knipe et al., 2013). IFNs induce numerous responses in the infected and surrounding cells, such as activation of the JAK/STAT kinase pathway and activation of other enzymes (Knipe et al., 2013). IFN-α also seems to inhibit α gene expression in the infected cells. Type I and II IFNs control the first wave of HSV gene expression during reactivation (Linderman et al., 2017). Apart from local cellular responses, IFNs also have immunomodulatory properties and induce local inflammation (Knipe et al., 2013). Of the recruited immune cells, natural killer cells are first responders that lyse the infected cells. Other first responders are macrophages that release immune cell mediators at the site of the infection, like interleukins (ILs). According to the authors, macrophages are important for antigen presentation and consequent antibody-dependent cellular toxicity. Moreover, dendritic cells mature at the infection site and travel to present antigens to naïve T cells in lymph nodes, priming them. Thus, HSV specific immune responses are formed, and following T cell priming, humoral antibody production begins, predominantly of the IgA type, followed by IgG, as suggested by Knipe et al.

1.2.7. Nonessential neurovirulence gene $\gamma_1$34.5

The nonessential neurovirulence gene $\gamma_1$34.5 of HSV encodes the neurovirulence factor ICP34.5, which accounts for virulence in humans (Knipe et al., 2013). The location of $\gamma_1$34.5 in the HSV genome is illustrated in **Figure 2**. Knipe et al. explain that the C-terminal domain of ICP34.5 inhibits protein kinase R that normally phosphorylates eukaryotic translation initiation factor 2 α during infection, and thus inhibits protein synthesis in the neuronal host cell. The N-terminal domain of the gene blocks autophagy of the infected cell by binding to the autophagy factor Beclin 1. The authors also explain that the $\gamma_1$34.5 gene also enables evasion of major histocompatibility complex class 2 responses. Further, it blocks the maturation of conventional dendritic cells and inhibits interferon signaling (Hukkanen and Seppänen, 2020). Thus, $\gamma_1$34.5 protects HSV from cellular responses. Deletion of this gene blocks HSV's ability to destroy neuronal cells, both its invasion and replication.

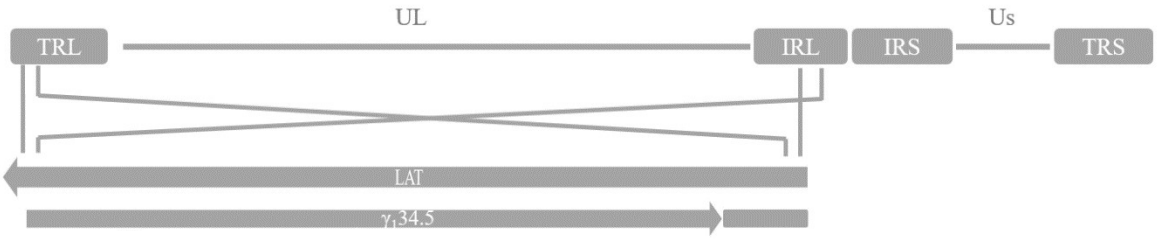

Figure 2. The location of γ134.5 in the HSV-1 genome. The γ134.5 gene has two domains in the unique long (U_L) component of the HSV-1 genome and is located opposite to LAT. The repeats are located in the terminal repeats of the long region (TRL) and internal repeats of the long region (IRL). Left to the long component is the unique short (U_S) component with internal repeats of the short region (IRS) and terminal repeats of the short region (TRS).

1.2.8. Disease models

There are animal models available that are used to study HSV infection pathogenesis and treatment. However, the fundamental problem is that HSV is strictly a human pathogen (Knipe et al., 2013). Still, many features of orofacial HSV infection can be replicated in mice, rats, and in rabbits. Furthermore, Knipe et al. stress that for the animal species and strain used, immune competence, as well as the viral strain and route of infection all influence the pathophysiology of the infection in the disease model, and may deviate from human infection. The authors also highlight another pressing issue with the current disease models of virulence and latency, that depending on the viral strain, the viral quantities used for inoculation may cause encephalitis in the model animal, which is fatal. For active infection, corneal or intranasal models are commonly used, whereas in a few models the abraded skin is inoculated with virus (Linehan et al., 2018). These models attempt to use natural routes of infection, and are useful in the development of antiviral therapies.

1.3. HSV as a viral vector

Most HSV-1 genes are in contiguous transcription units as a single copy, making them suitable for easy manipulation for the construction of viral vectors (Diefenbach and Fraefel, 2020). HSV-1 is exploited as a gene delivery vehicle for the development of gene therapy, as its genes can be altered or removed and transgenes added without drastically affecting virus production in cultured cells. It also possesses a broad host range with the ability to infect both nondividing and dividing cells. According to Diefenbach and Fraefel, replication defective viruses are unable to reactivate from latency but may still express transgenes long-term through the latency viral promoter system. These features make HSV-1 suitable as a vector.

1.3.1. Vectors with $\gamma_1$34.5 deletion

The most common HSV-1 viral vectors have a neurovirulence gene $\gamma_1$34.5 deletion and are conditionally replicative.

The $\gamma_1$34.5 gene deleted vector requires over 3000-fold plaque forming unit (pfu) dosage for neurovirulence compared to wild type viruses (Whitley et al., 1993). Withley et al. argue that the vector is the least virulent mutant of HSV known. If the transgene is located under the latency-associated promoter, its expression in nervous systems has been observed 6 months after infection according to a study by Broberg et al. (2004). Existing immunity does not affect HSV-mediated gene transfer in animal models or in humans (Andtbacka et al., 2015). Broberg et al. (2004) demonstrated that the vector can spread throughout the central nervous system but does not cause tissue destruction.

Vectors with a $\gamma_1$34.5-deletion can still replicate in tumor cells as the interferon pathways are often defective in these cells (Hukkanen and Vihinen, 2016). HSV-1 vectors with a $\gamma_1$34.5 deletion have been proven safe and efficacious in clinical trials, as talimogene laherparepvec (T-vec), a HSV-1 vector, was approved in 2015 by the U.S. Federal Drug Administration and the European Medicines Agency for intratumoral injections for the treatment of metastatic melanoma. T-vec also has a deletion of the α47 gene, a gene involved with immune evasion. However, the efficacy of T-vec in the treatment of melanoma is dependent on the host's own immune response against the tumor, and thus a transgene of GM-CSF cytokine is inserted into the vector. This gene stimulates the host immunity to the infected tumors.

1.3.2. Production of HSV vectors

The selection methods used to purify HSV-1 vectors from the parental HSV-1 are scarce, and often tedious. As HSV-1 forms microscopic plaques *in vitro*, one commonly used method is plaque purification, with the use of a marker gene that enables selection. This could be a gene expressing green fluorescent protein (GFP), β-galactosidase or luciferase (Goins et al., 2020). Plaques are identified using a fluorescent microscope and then picked. This method is tedious and may require multiple plaque purifications for a successful selection, as the parental virus usually grows more efficiently than the vector.
A traditional method for purification is using selection for and against thymidine kinase (Roizman and Jenkins, 1985). TK is deleted in the recombinant vectors, rendering the intermediate vector resistant to acyclovir treatment. Thus, acyclovir treatment of the cells stops the growth of parental TK positive viruses, while TK negative recombinants can continue replicating. For the safe use of these viral vectors, the purified vectors must be reinserted with TK, and purified again. Obstructing the thymidylate synthetase pathway with HAT medium containing hypoxanthine, aminopterine and thymidine depletes TK-deficient recombinants. However, TK negative recombinants survive a few days in HAT medium while TK positive recombinants might not grow sufficiently. This is why TK selection requires multiple consecutive selections in order to purify the vector.
Bacterial artificial chromosome (BAC) technology is a method that circumvents the laborious purifications the previous methods require. The viral genome can be contained in an episome in bacterial cells, and thus cloned without requiring eukaryotic cells (Falko and Weir, 2006). This BAC-cloned viral DNA can after mutagenesis be transfected into a cell line and generate recombinant viral particles. BAC cloning can however be difficult, requiring special bacterial strains and numerous steps.

1.4. RNA interference

RNA interference is a cellular mechanism of gene silencing in eukaryotic cells first described by Fire et al. 1998. The mechanism is activated when double-stranded RNA is cleaved by Dicer into small fragments called small interfering RNA (siRNA), which prime a gene silencing enzyme complex which inhibits the protein synthesis of the specific gene (Bhuyan et al., 2004). RNA interference was first discovered in plants as an antiviral mechanism, and now describes all RNA-induced gene silencing mechanisms.

The mechanism of RNA-induced gene silencing begins with either the Dicer cleaved siRNAs or exogenous siRNA binding to the Dicer-2/R2D2 complex (Rand et al. 2005). This complex enables RISC complex formation, in which the guide RNA strand gets loaded onto Argonaute 2. RISC then uses the guide RNA to find the complementary messenger RNA via base pairing and cleaves the target molecule, inhibiting translation.

Not only does exogenous siRNA have potential to be used therapeutically, but it is also an excellent tool for simple knockdown of a gene of interest within research laboratories. Several experimental siRNA therapies have been developed, for indications ranging from viral infections, such as hepatitis B, to cancer, such as gliosarcoma (Javanbakht et al., 2018; Hwang et al., 2016). However, the serum instability of administered siRNA is the main issue regarding systemic therapeutic use.

1.4.1. Inhibition of HSV-1 using RNA interference

Studies of the application of siRNAs for the successful inhibition of HSV infections *in vitro* have been reported. There are also reports of successful reduction of clinical signs of HSV infections in rodents. All of these studies report using siRNA treatment that target the replication of the virus.

Jin et al. (2014) targeted the capsid proteins encoded by U_L19 and U_L18 of HSV-1 and found that the siRNA greatly interfered with the formation of the viral capsid. This was reflected in a successful inhibition of viral replication *in vitro*.

Similarly, Zhang et al. (2008) targeted α-TIF and DNA polymerase and successfully inhibited HSV-1 replication *in vitro*. Song et al. (2016) also demonstrated efficacy *in vitro* in the replication of HSV-1 using siRNA targeting the genes U_L29 and U_L28, which had previously been proven efficacious in the treatment of lethal HSV-2 infection by Palliser et al. (2006) in mice.

Silva et al. (2014) targeted the U_L39 gene and successfully inhibited 99% of HSV-1 replication *in vitro*. These siRNAs were further tested in the treatment of HSV-1 encephalitis in mice (Silva et al., 2016) with a significant reduction in clinical signs of infection, and an inhibition of replication of HSV-1 in the brain and trigeminal ganglia of the mice. The study, however suffered from imprecise quantitation of the antiviral efficacy.

These studies show that RNA interference can successfully be used in research laboratories to prevent the replication of HSV-1 both *in vitro* and *in vivo*. They also show that the development of RNA interference into a therapeutic treatment against HSV-1 is promising. Still, the instability of siRNA in serum and the possibility of point mutations remains a challenge to overcome. However, the development of siRNA swarms, i.e. large pools of siRNAs cleaved from a long double-stranded RNA precursor, can circumvent possibilities of point mutations of the target potentially rendering single siRNAs ineffective. These swarms have been proven efficacious against HSV-1 both *in vitro* and *in vivo* (Romanovskaya et al., 2012; Paavilainen et al., 2015, 2016, 2017; Levanova et al., 2020; Kalke et al. 2020).

1.5. Summary

HSV-1 is a versatile virus that can either cause severe disease or be utilized to treat serious conditions, as in the case of T-vec. As there is no cure or vaccine available for HSV-1 infections, there is a medical need to develop new treatments that could either prevent or cure the infection. Furthermore, the field of herpesviral vectors and oncolytic viruses is rapidly expanding. A new purification method that would be straightforward and less time-consuming would accelerate the research. As antiviral siRNA has been proven simple yet effective in use both *in vitro* and *in vivo* in research laboratories, interest in the effects of targeting nonessential genes in HSV has arisen. It is interesting to observe whether the targeting of the nonessential neurovirulence gene $\gamma_1$34.5 of a wild type virus would change the viral phenotype to that of a $\gamma_1$34.5-deleted vector. This could be applied to vector production, to retarget viral replication or possibly deplete the parental virus during plaque purification. Furthermore, this treatment could possibly be applied to protect animals in rodent models from severe disease and early death. In this Master's thesis, six siRNAs targeting $\gamma_1$34.5 were tested *in vitro* to see whether targeting $\gamma_1$34.5 has any antiviral potential, or potential to be developed further into uses in infection models or viral purification protocols.

2. Results

2.1. Effects of g345 siRNAs on cell viability

The cytotoxicity of the synthesized siRNAs and the transfection reagent were assessed in both MG and HCE cells. The cell viability was assessed with three different amounts of siRNA per well (1, 5, and 10 pmols). Please refer to Materials and methods sections 4.4 and 4.7 for clarification of the methods used, and section 4.1 and 4.2 for the siRNAs and cells used. The cellular viability of the siRNA treated cells of all three concentrations were similar to that of cells only-controls, which were left untreated, and mock controls, which were treated only with the transfection reagent RNAiMAX and no siRNA (**Figure 3**). There is some insignificant variation between the treatments. Most of the siRNA treatments have a cellular viability of 80-120% compared to cells only and mock, with the largest variation in MG cells (**Figure 3A**). The positive toxic control 88bp (a treatment of 1 pmol/well) caused a significant ($p<0.05$) decrease of cellular viability of 65% in both cell lines.

2.2. Transfectability of HCE and MG cells

To assess the transfectability of the cell lines, a negative control Sic-003 (nonspecific siRNA with a fluorescent cyanine 3 modification) and a positive toxic control (88bp) were used. After transfection, images were taken with EVOS using a RFP filter 48 hours post transfection. As shown in **Figure 4**, MG cells had visually taken up more Sic-003 than HCE cells. Due to these observed visual differences between the cell lines, HCE cells were further examined. Two parallel experiments were conducted, one where HCE cells were transfected, and one where the HCE cells were first infected and then transfected, to assess whether infection improves transfectability. The cells were monitored using EVOS at multiple time points. Visually, there was little difference between non-infected cells and infected cells (images not shown). However, it can be noticed that a lot of siRNA-lipofectamine complex debris is adhered to the bottom of the well and seems to be adhered onto the surface of the cells even after washing (**Figure 3**). This debris decreased in amount after some time.

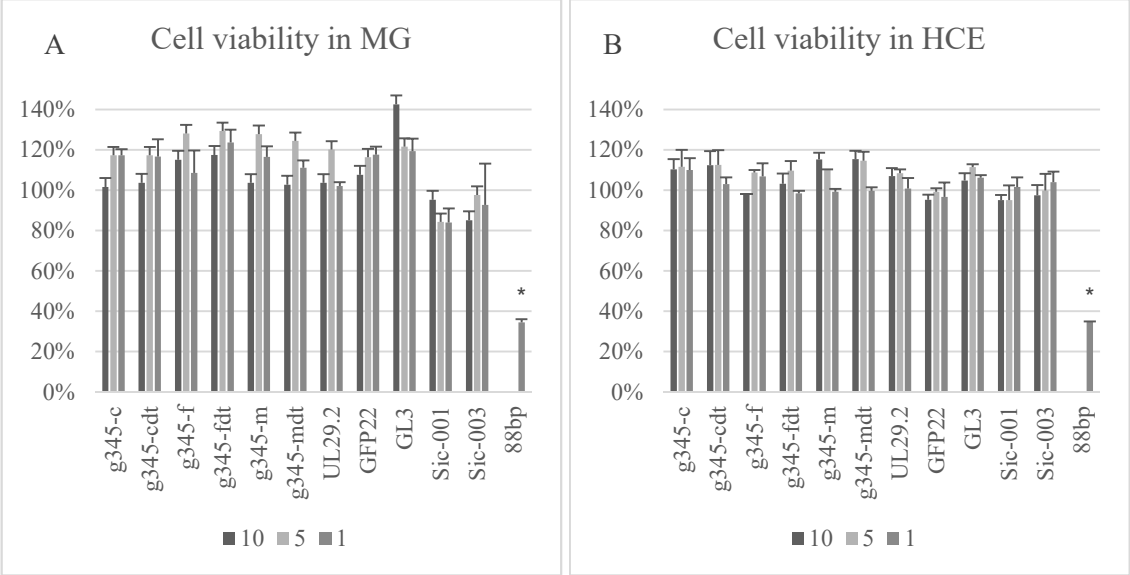

Figure 3. Cell viability of MG and HCE siRNA treated cells. A. The relative cell viability in MG cells. B. The relative cell viability in HCE cells. The columns represent cells transfected with 1, 5 and 10 pmols of siRNA per well respectively, or with 1 pmol of the positive toxic control 88bp per well. Cells only control was untreated and mock control was treated with transfection reagent only. The relative viability is presented as the percentage of the mean of cells only and mock. The whiskers above the bars represent the standard deviation of the mean. The p-values of each treatment are calculated against cells only and mock (* $p<0.05$).

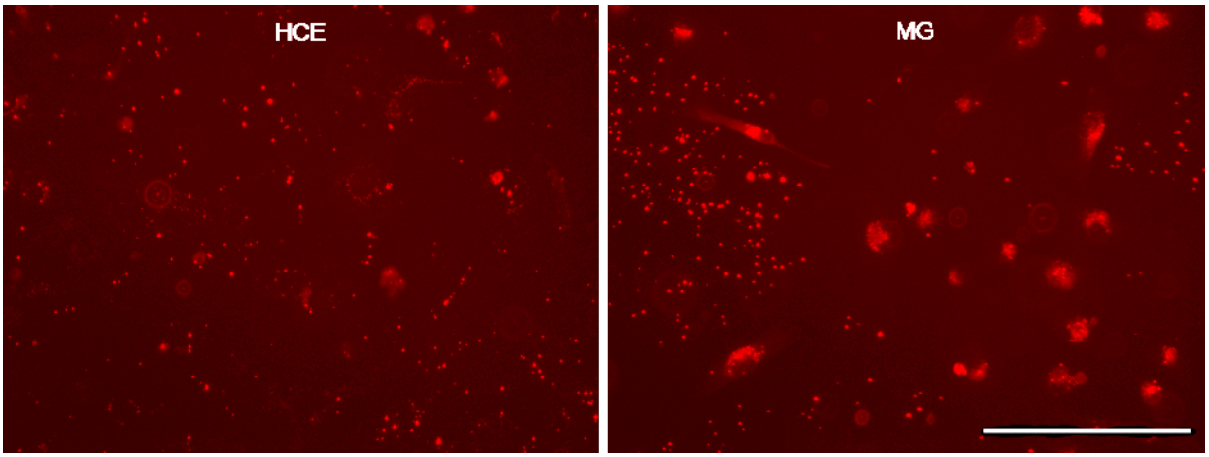

Figure 4. HCE and MG cells transfected with fluorescent nonspecific siRNA. The images show cells transfected with 20 pmols of siRNA per well and imaged 48h post transfection. The picture on the left represent HCE cells and the picture on the right MG cells. The bright, small crystal shaped siRNA is debris that has adhered to the bottom of the well and possibly on top of the cells, while the bright red shadows represent the transfected siRNA. The scale bar represents 200µm.

2.3. Growth rates of LoxGFP versus H1052

The differences in growth rate of the wild type-like virus LoxGFP and the vector backbone H1052 was monitored and documented in HCE and MG cells using an EVOS fluorescent microscope. For clarification of viruses used, please refer to Materials and methods section 4.3, and for methods used, please refer to Materials and methods sections 4.5 and 4.9.

H1052 expresses its marker transgene significantly slower than LoxGFP in both cell lines. LoxGFP-infected cells reached a CPE (cytopathic effect) of 75% at day 2 (24h post infection) and a CPE of 100% at day 3 (48h post infection), while H1052 seemed to reach 75% CPE at day 5 (96h post infection) (**Figure 5A**). At days 4 and 5, the LoxGFP - infected HCE cells seemed to undergo lysis.

The amount of virus in the supernatant was quantified using plaque titration. On day 3 there is almost a hundred-fold difference in viral titers in the supernatant between the two virus types in both cell lines (**Figure 5C**). The titers also reflect the amount of virus that the cells were infected with, however, at day 3 it seems that 10 000 and 1 000 pfu of LoxGFP yield similar viral shedding. Furthermore, 1 000 or 100 pfu of H1052 have an equal impact. When comparing the viral shedding of H1052 at different time points, in most cases there has been a ten-fold increase in the titer after two days (**Figure 5B**). This is not the case in the wells infected with 10 000 pfu of virus, which in MG cells causes a decrease in the viral titer and in HCE cells yields a similar titer.

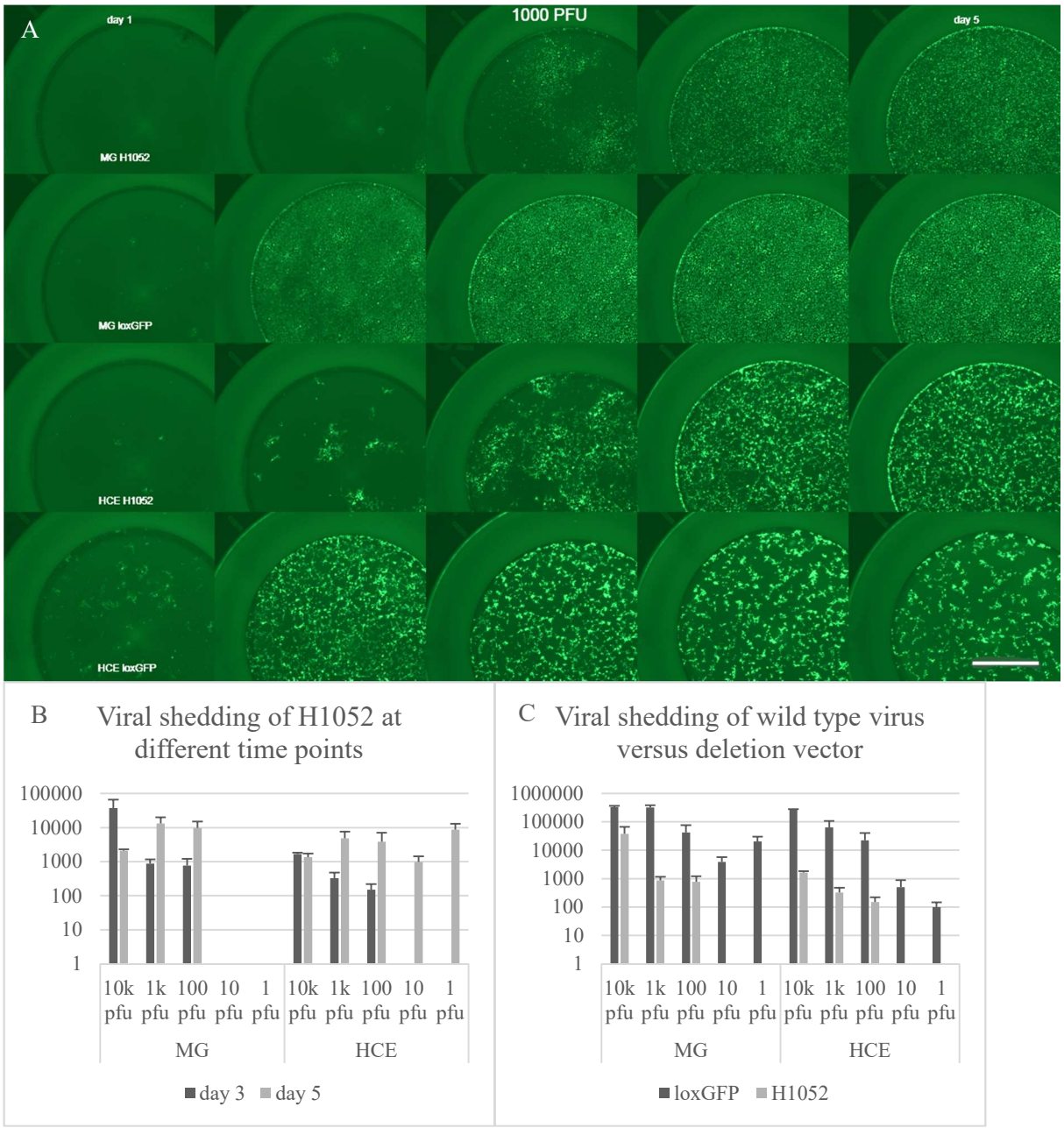

Figure 5. Viral growth of H1052 and LoxGFP in HCE and MG cells. A. HCE and MG cells infected with 1 000 pfu per well and imaged for five consecutive days using EVOS fluorescent microscope, with a GFP filter. Infected cells express the marker gene GFP. Day 1 represents the day of infection (0h), and day 5 represents 96h post infection. B. Viral shedding quantification of H1052 in HCE and MG cells during the growth monitoring experiment. HCE and MG cells infected with 10 000, 1 000, 100, 10 and 1 pfu per well. The results show viral shedding of H1052 into the supernatant on day 3 and 5. C. Viral titers of LoxGFP and H1052 from the same setting as B on day 3. The whiskers above the columns represent the standard deviation. The scale bar represents 2000 µm.

2.3. Antiviral efficacy of g345 siRNAs

Antiviral assays were conducted to assess whether the siRNAs have antiviral properties when used on the wild type-like virus LoxGFP. For clarification on the methods used, please refer to Methods and materials sections 4.5, 4.6 and 4.8.

In MG cells, there is a visual reduction in GFP expression in infected g345-m and g345-f treated cells compared to untreated infected cells (**Figure 6**). There is also an increase in GFP expression in g345-c and g345-cdt treated cells, while GFP expression is absent in UL29.2 and 88bp treated cells.

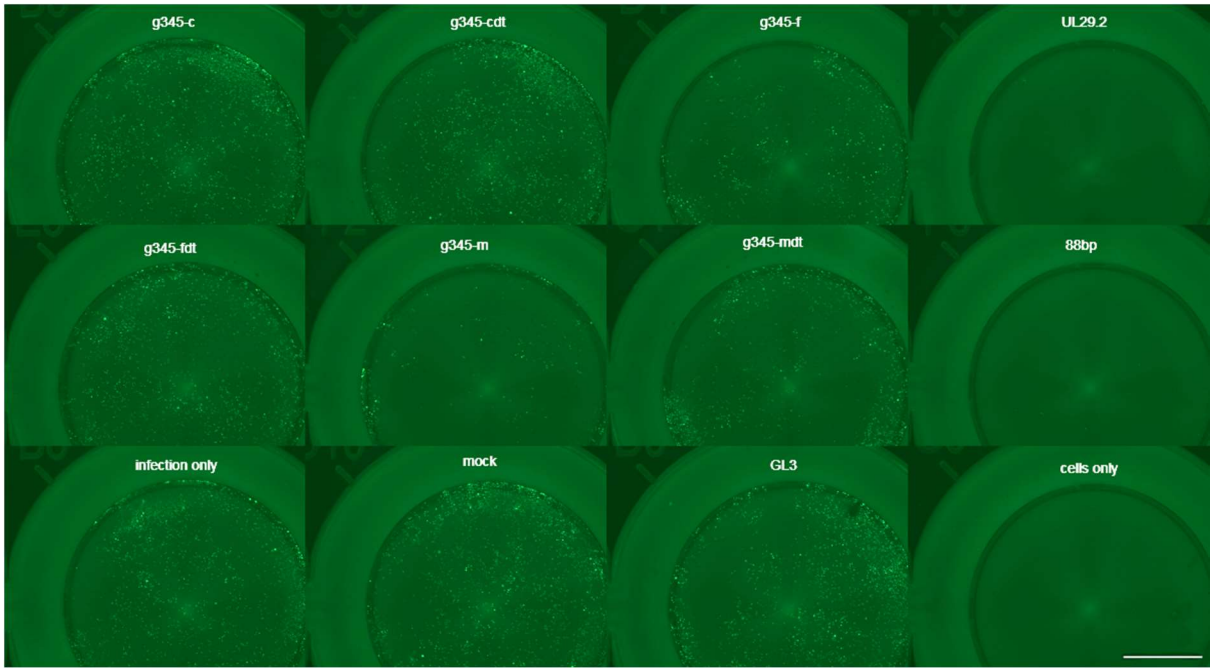

Figure 6. Antiviral efficacy of g345 siRNAs in MG cells. MG cells transfected with 10 pmols of siRNA per well and later infected with 1 000 pfu of LoxGFP. Infected cells express the marker gene GFP. The images were taken 48h post transfection using EVOS. The scale bar represents 2000 µm.

2.3.1. Effects of siRNA treatment on viral shedding

To determine antiviral efficacy of the siRNA treatment, the viral shedding was determined by quantifying the titer of the supernatant using plaque titration, with the plaques counted after staining. For clarifications on the methods used, please refer to Materials and methods section 4.9.

In all three cell lines a successful transfection can be observed. There is a significant decrease ($p<0.05$) in the titer in the known antiviral UL29.2 treated samples compared to infection only (**Figure 7**). The toxic control 88bp treated samples show a decrease in viral shedding in MG and HCE cells (**Figures 7A** and **7B**). The toxic control 88bp induced no

decrease in viral shedding in Vero cells (**Figure 7**). In GL3 treated Vero cells, a significant decrease in titer can be observed. The infected control treated with transfection reagent (mock), infected GL3 nonspecific control, and the infection only untreated control samples showed no statistically significant variation.

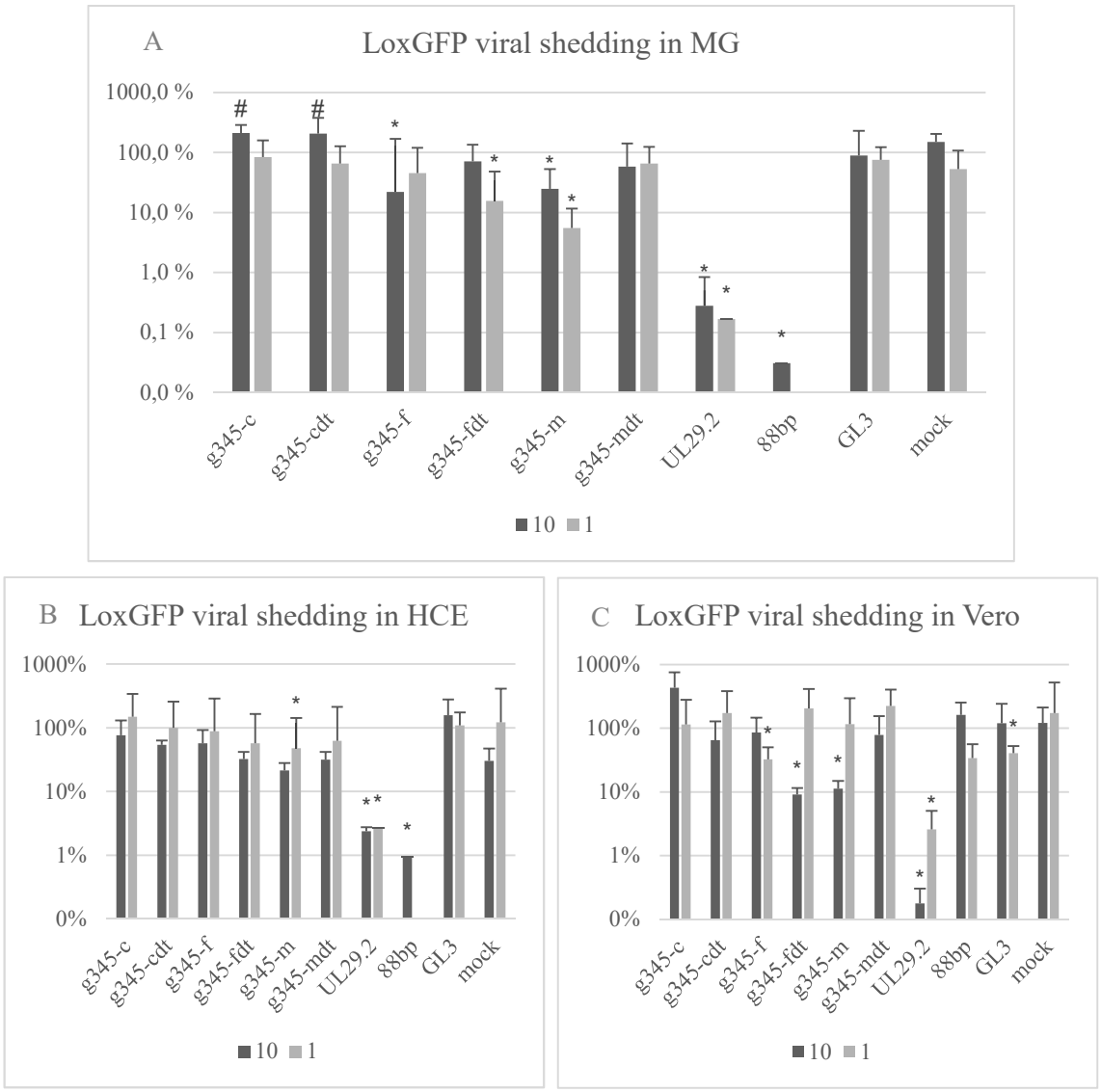

Figure 7. Viral shedding of LoxGFP in the antiviral assays. The viral shedding of the wild type virus LoxGFP to the supernatant during the antiviral assays is presented. A. Viral shedding in MG cells. B. Viral shedding in HCE cells. C. Viral shedding in Vero cells. The titers are presented as pfu/ml and normalized to their respective untreated infection only control. Groups 10 and 1 represent the respective antiviral assay plates of the g345 siRNA treatment at 10 and 1 pmol/well. The antiviral assays were infected with 1 000 pfu per well, and the supernatant collected 48 hours post transfection. The p-values were calculated against their respective infection only samples, with an increase in titer (# $p<0.05$) or a decrease in titer (* $p<0.05$). The whiskers above the columns represent the standard deviation.

Cells treated with g345-m siRNA show a decrease in the viral titer in all three cell lines, although the significant decreases seem not to follow a trend in relation to the amount of siRNA used. G345-m induces a significant reduction in viral shedding in MG cells and Vero cells at 10 pmol/well, as well as in MG cells and HCE cells at 1 pmol/well. Cells treated with 10 pmol/well of g345-f and g345-fdt induced a decrease in viral shedding in MG cells and Vero cells respectively, and g345-f and g345-fdt at 1 pmol/well reduced viral shedding in Vero cells and MG cells respectively. The g345-c and g345-cdt treated samples have a significant increase in viral shedding ($p<0.05$) in MG cells (**Figure 7A**). The antiviral assay and titration in MG cells using 10 pmol/well was repeated, and similar results were acquired (data not shown.)

2.3.2. Effects of siRNA treatment on α-TIF and $\gamma_1$34.5 gene expression

To confirm whether the g345 siRNAs inhibit $\gamma_1$34.5 gene expression, or even inhibit the replication of the virus, reflected by α-TIF gene expression, the gene expressions of the LoxGFP antiviral assays were quantified using quantitative real-time PCR (q-RT-PCR) and normalized to each sample's respective GAPDH expression. The normalized data was then further normalized to the respective infection only control. For methods used, please refer to Materials and methods sections 4.10, 4.11 and 4.12.

In all of the cell lines, the cells treated with the known antiviral control UL29.2 show a significant decrease ($p<0.05$) in both α-TIF gene expression and $\gamma_1$34.5 compared to infection only (**Figure 8**). Furthermore, the cytotoxic control 88bp also shows a decrease in the α-TIF and $\gamma_1$34.5 gene expression in HCE and MG cells, but shows no significant difference in Vero cells compared to infection only. The expression of $\gamma_1$34.5 in Vero cells treated with 1 pmol/well of nonspecific GL3 shows a significant decrease (**Figure 8F**), which is reflected in the titration (**Figure 7C**).

For the g345 siRNAs, 10 pmol/well treated cells all have a significant decrease ($p<0.05$) in the gene expression of $\gamma_1$34.5 in MG cells compared to infection only (**Figure 8B**). For the 1 pmol/well treated cells there is a slight decrease, however due to variation in the samples it is not statistically significant. MG cells treated with 10 pmol/well of g345 siRNA show a significant decrease in expression compared to infection only, except for g345-cdt (**Figure 8A**). Furthermore, cells treated with 1 pmol/well of g345-fdt and g345-m also show a significant decrease in gene expression.

In HCE cells, there is no significant decrease in either α-TIF or $\gamma_1$34.5 gene expression compared to infection only, while cells treated with 10 pmol/well of g345-mdt show a

significant increase ($p<0.05$) in $\gamma_1$34.5 gene expression compared to infection only (**Figure 8D**). A similar observation can be seen in the expression in Vero cells, where a decrease seen in α-TIF gene expression with g345-fdt at 10 pmol/well and $\gamma_1$34.5 gene expression with g345-fdt 1 at pmol/well (**Figures 8E** and **8F**).

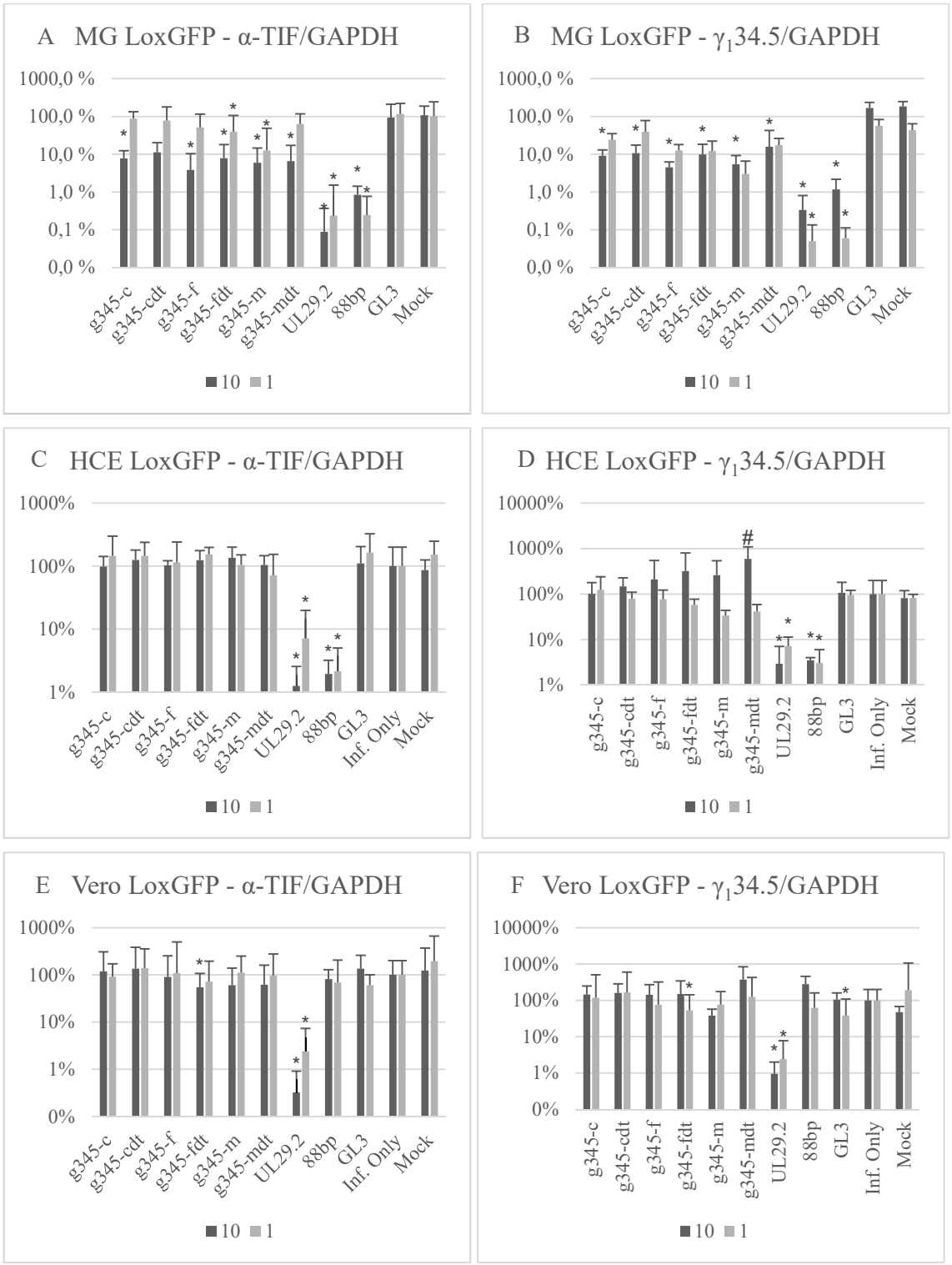

Figure 8. Gene expression of α-TIF and $\gamma_1$34.5 in siRNA treated cells. The gene expression of α-TIF and $\gamma_1$34.5 was quantified from the antiviral experiments using q-RT-PCR and normalized to GAPDH, and further normalized to the respective infection only control. A. Expression of α-TIF in LoxGFP infected siRNA treated MG cells. B. Expression of $\gamma_1$34.5 in LoxGFP infected siRNA treated MG cells. C. Expression of α-TIF in LoxGFP infected siRNA treated HCE cells. D. Expression of $\gamma_1$34.5 in LoxGFP infected siRNA treated HCE cells. E. Expression of α-TIF in LoxGFP infected siRNA treated Vero cells. F. Expression of $\gamma_1$34.5 in LoxGFP infected siRNA treated Vero cells. In the figure groups 10 and 1 represent the respective antiviral assay plates of the g345 siRNA treatment at 10 and 1 pmol/well. The p-values were calculated using the GAPDH normalized value against the respective infection only GAPDH normalized value with an increase (# $p<0.05$) or a decrease (* $p<0.05$). The whiskers above the columns represent the standard deviation.

2.3.3. Effects of siRNA treatment on innate responses

To examine how the g345 siRNA treatment affects the innate immunity of infected cells, interferon stimulated gene factor (ISG) 54, IFN-β and IL-29 gene expression was quantified. Each sample was normalized to its respective GAPDH expression and then further normalized to the cytotoxic control 88bp. In both cell lines ISG54, IFN-β and IL-29 expression was significantly decreased ($p<0.05$) in cells treated with 88bp compared to infection only (data not shown).

The ISG54 expression in HCE cells treated with 1 pmol/well g345-m or UL29.2 shows a significant increase ($p<0.05$) compared to infection only (**Figure 9A**). In MG cells treated with 10 pmol/well of g345-c or g345-cdt, there is a significant decrease in expression compared to infection only (**Figure 9B**). MG cells treated with 10 pmol/well of g345-f or UL29.2, 1 pmol/well of g345-m and mock treated cells from the 10 pmol setting show a significant increase in expression.

IFN-β expression is significantly increased in HCE cells treated with 10 pmol/well of g345-m or g345-mdt (**Figure 9C**). There is no other significant increase or decrease in IFN-β expression in HCE or MG cells. In MG cells treated with 10 pmol/well of g345-c, there is no detectable IFN-β expression (**Figure 9D**).

In HCE cells treated with 10 pmol/well of g345-cdt, there is an increase in IL-29 expression (**Figure 9E**). The treated MG cells lack detectable expression of IL-29 in cells treated with 10 pmol/well of g345-c, g345-cdt, g345-mdt, and infection only, as well as 1 pmol/well of g345-cdt, g345-f, g345-mdt, GL3, infection only, and mock (**Figure 9F**). There is a statistically significant increase of IL-29 in MG cells compared to infection only in cells treated with 10 pmol/well of g345-f or UL29.2, while the other samples showed no statistically significant difference.

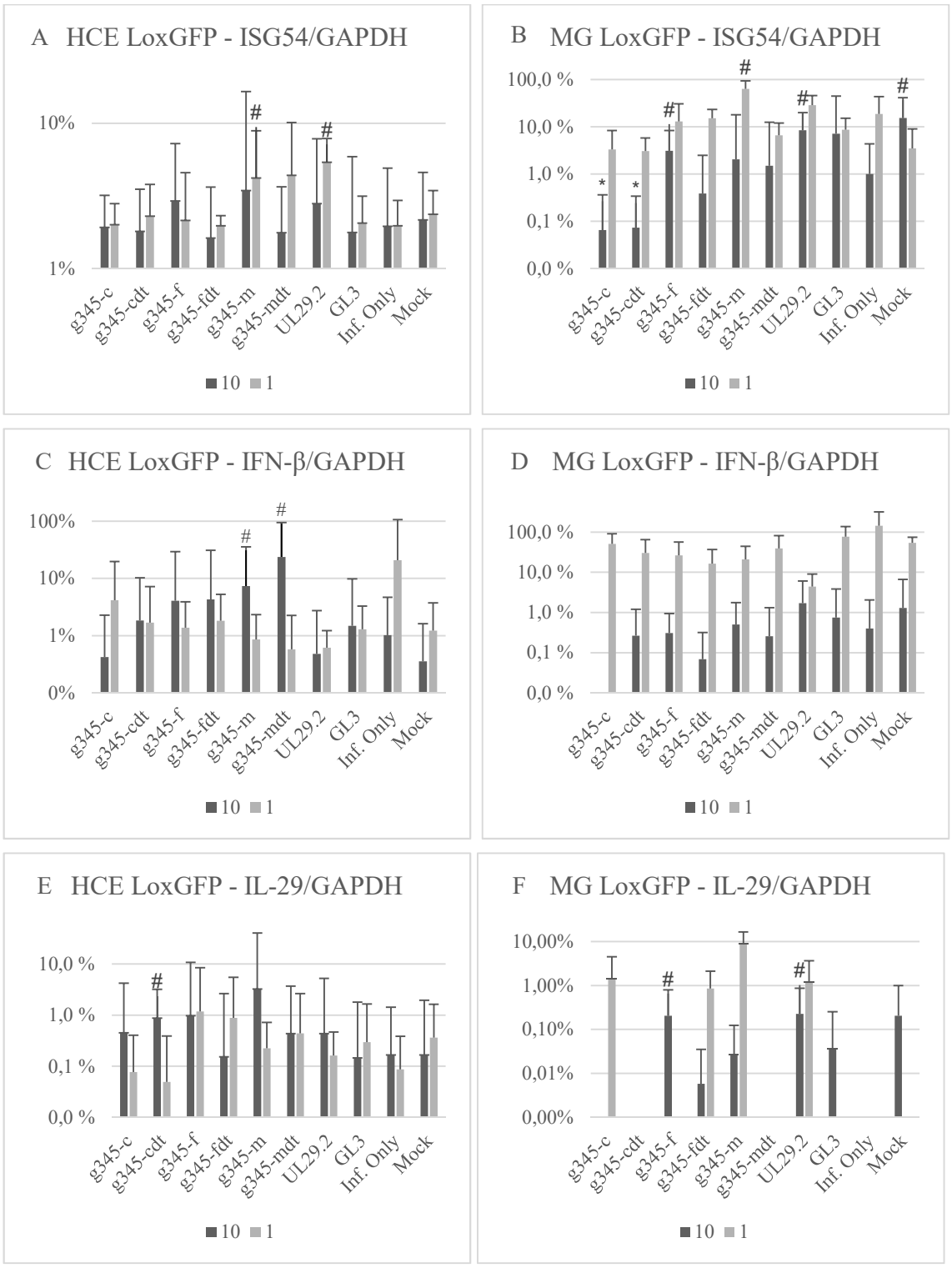

Figure 9. ISG54, IFN-β and IL-29 expression in siRNA treated HCE and MG cells. The gene expression of ISG54, IFN-B and IL-29 was quantified from the antiviral experiments using q-RT-PCR and normalized to GAPDH, and further normalized to the respective 88bp cytotoxic control. A. Expression of ISG54 in LoxGFP infected siRNA treated HCE cells. B. Expression of ISG54 in LoxGFP infected siRNA treated MG cells. C. Expression of IFN-β in LoxGFP infected siRNA treated HCE cells. D. Expression of IFN-β in LoxGFP infected siRNA treated MG cells. E. Expression of IL-29 in LoxGFP

infected siRNA treated in HCE cells. F. Expression of IL-29 in LoxGFP infected siRNA treated MG cells. Groups 10 and 1 represent the respective antiviral assay plates of the g345 siRNA treatment at 10 and 1 pmol/well. The p-values were calculated using the GAPDH normalized value against the respective infection only GAPDH normalized value with an increase (# $p<0.05$) or a decrease (* $p<0.05$). The whiskers above the columns represent the standard deviation.

2.4. Effect on viral shedding of H1052

To determine antiviral efficacy of the siRNA treatment on H1052, antiviral assays identical to that of LoxGFP were conducted in MG cells.

There was a statistically significant increase ($p<0.05$) of viral shedding in MG cells treated with 10 pmol of g345-cdt per well compared with infection only (**Figure 10**). All of the samples treated with 1 picomole of siRNA per well (except for g345-fdt) and the respective mock had significantly decreased ($p<0.05$) viral titer compared with infection only (**Figure 10**).

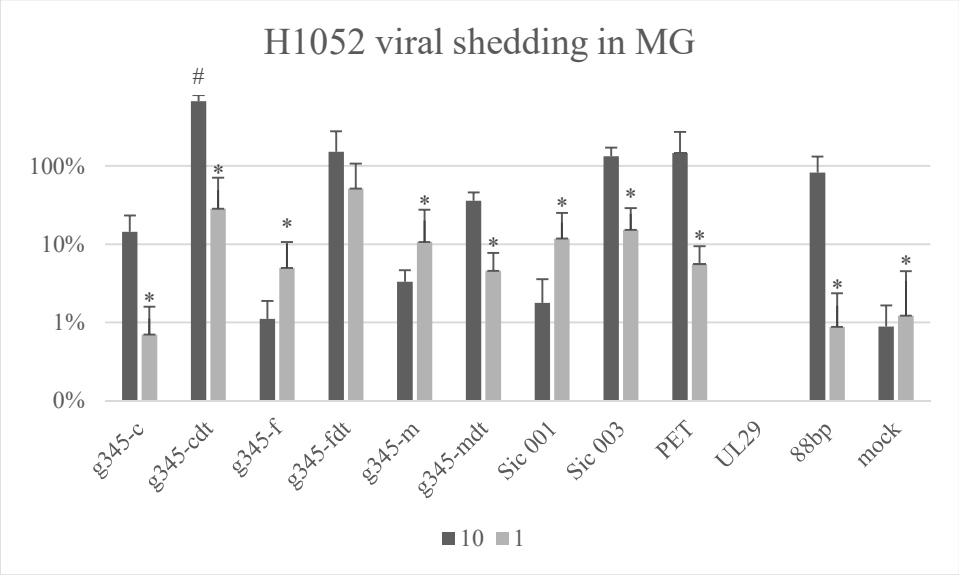

Figure 10. Viral shedding of H1052 in siRNA treated MG cells. The graph represents the viral shedding of the vector backbone H1052 to the supernatant in the antiviral assay quantified using plaque titration. The titers are determined in pfu/ml and normalized to their respective infection only, which is untreated. In the figure, groups 10 and 1 represent the respective antiviral assay plates of the g345 siRNA treatment at 10 and 1 pmol/well. The antiviral assays were infected with 1 000 pfu per well, and the supernatant collected 48 hours post transfection. The p-values were calculated against their respective infection only, with an increase in titer (# $p<0.05$) or a decrease in titer (* $p<0.05$). The whiskers above the columns represent the standard deviation.

3. Discussion

All previously published studies of RNA interference against HSV have targeted essential genes of the HSV genome. Although proven successful in experimental settings both *in vitro* and *in vivo*, studies of RNA interference against HSV-1 remain few. Interest has arisen whether targeting nonessential genes of HSV could be developed for experimental settings, and what effect it would have on the phenotype of the virus.

The objective of this thesis was to investigate whether targeting the nonessential neurovirulence gene $\gamma_1$34.5 using RNA interference is antiviral or gene specific, changing the phenotype of the wild type virus to that of the viral vector. Additionally, the effects of $\gamma_1$34.5 interference on the innate responses were studied.

Six siRNAs targeting $\gamma_1$34.5 were assessed in this study, two within the deletion region of $\gamma_1$34.5 in viral vectors and one outside, each with a corresponding dTdT modification to assess whether the modification influences the choice of target strand.

First, cytotoxic assays in MG and HCE cells were conducted. Following this was an antiviral study using a prophylactic model of transfecting cells with siRNA followed by infection with a wild type-like virus. From these antiviral studies, the viral shedding to the supernatant was quantified. Because $\gamma_1$34.5 is a nonessential gene, the quantification of viral shedding does not confirm whether successful inhibition of the gene has occurred, thus the RNA was extracted from the treated cells, converted to cDNA and q-RT-PCR performed.

Initially, gene expression of α-TIF, which reflects the replication of virions in the host cell, and $\gamma_1$34.5, which is the gene inhibited by the siRNA, were quantified. The innate responses ISG54, IFN-β and IL-29 were also quantified in the host cells from the same samples. It was hypothesized that the inhibition of $\gamma_1$34.5 would restore the host cell's response to an infection and increase the gene expression compared to infected, untreated samples.

The antiviral study was repeated using the vector backbone, to assess whether the siRNA treatment was antiviral even in the $\gamma_1$34.5 deleted virus. This study was only done in the cell line which had the most promising results from the previous study.

3.1. The g345 siRNA do not induce cytotoxic responses *in vitro*

For the cytotoxicity assays the HSV susceptible cell lines MG and HCE were chosen, representing nervous tissue and epithelial tissue respectively. MG cells have previously been used in HSV-1 siRNA swarm publications and have proven transfectability (Paavilainen et al. 2015, 2016; Romanovskaya et al. 2012). The cytotoxicity assays were not performed in Vero cells, as they lack interferon signaling and the cytotoxic control 88bp fails to induce cytotoxicity.

Successful transfection in both cell lines was measured by a significant decrease in the viability after 48 hours in cells treated with the cytotoxic control 88bp, which showed a 65% decrease in cellular viability compared to untreated cells and cells treated with transfection reagent only (mock) (**Figure 3**). The viability was determined using a luminescent assay measuring cellular adenosine triphosphate levels (Romanovskaya et al., 2012).

In contrast to previous publications (Levanova et al., 2020), the transfection reagent does not induce any cytotoxicity in this study. The values were similar to that of untreated samples, hence why their average was combined to normalize the siRNA treated samples. There is however a nonsignificant variation between the siRNA treated samples and the untreated samples, possibly due to the positioning on the plate. Furthermore, the varying cellular viability does not follow a trend regarding the amount of picomoles used, or whether the siRNA is modified or not.

Thus, it can be concluded that the siRNAs induce no toxicity in MG and HCE cells, at the amounts of 1, 5, and 10 picomoles per well. Furthermore, there is no observable or statistical difference between non-modified siRNAs and siRNAs with dTdT modification.

3.2. HCE cells might have low transfectability

In relation to the cytotoxicity assays, both HCE and MG cells transfected with a luminescent cyanine 3 modified siRNA, Sic 003, were imaged. There was a stark contrast between the cell lines, MG cells being bright red and easily noticeable, while HCE transfected cells were difficult to observe (**Figure 4**). There was no difference in the confluency between the cell lines when viewed in transmitted light. Furthermore, there seemed to be a lot of debris, presumably the siRNA-lipofectamine complex, adhered to the bottom of the well and the surface of the cells even after washing.

This raised the question as to whether infection would increase transfectability in HCE cells. HCE cells were either transfected with Sic 003, or infected with LoxGFP and later

transfected with Sic 003. The cells were imaged at different time points, however it was difficult to observe any visual differences, especially as the different fluorescent signals contaminated each other. Yet, it was observable that the Sic 003 transfection remained faint in the microscope, compared to the MG cells in the previous experiment.

3.3. H1052 and LoxGFP replicate in MG and HCE cells, but at different rates

It is evident from the viral growth experiment that both the wild type-like virus and the vector backbone replicate successfully in MG and HCE cells. However, the vector back bone replicates at a much slower rate in both neuronal cells and highly differentiated cells, as observed in this study. These results support previous studies done *in vivo* that show that delta gamma 34.5 replicates slowly in neuronal cells (Whitley et al., 1993; Broberg et al., 2004). The assessment was done based on levels of GFP expressed in infected cells. We have earlier established the association between marker gene expression and productive viral infection (Levanova et al., 2020). At 48 hours post infection, the differences in viral shedding to the supernatant between LoxGFP and H1052 varies between tenfold to a hundredfold (**Figure 5C**). H1052 only reaches a CPE of 75% on day 5, while LoxGFP reaches a CPE of 100% on day 2 (**Figure 5A**).

3.4. The g345 siRNAs induce varying amounts of viral shedding in MG cells

To assess whether $\gamma_1$34.5 inhibition using RNA interference is antiviral, the supernatants were collected from the prophylactic antiviral experiments and viral shedding was quantified using plaque titration. Vero cells were included as they are cells commonly used in vector production. The known antiviral control UL29, proven antiviral by Palliser et al. (2006), showed that the transfection had been successful in all cell lines used, while the cytotoxic control 88bp proved a successful transfection in MG and HCE cells.

The viral shedding of the different g345 treated infected MG cells varied significantly (**Figure 7A**). Surprisingly, the siRNAs g345-c and g345-cdt at 10 pmol/well induced a stark increase in viral titers. Therefore, the antiviral experiment and viral shedding quantification was repeated. The repeated experiment yielded similar results. Such a significant increase in viral shedding might be caused by the g345-c and g345-cdt siRNAs targeting a nonspecific gene in the host cell. However, g345-m induced a significant decrease in viral shedding in both 1 and 10 pmol/well treated cells, suggesting that g345-

m has antiviral properties. The corresponding g345-mdt siRNA failed to induce any significant antiviral effect in the treated cells, suggesting that the dTdT modification affects the choice of target strand. The siRNAs g345-f at 10 pmol/well and g345-fdt at 1 pmol/well also had antiviral efficacy, but interestingly there seems to be no correlation with the amount of siRNA used. Presumably 10 pmol/well of g345-fdt would induce the same or a greater result than 1 pmol/well, yet it failed to do so.

Altogether, these results show that g345-m is a promising siRNA, as it reduced viral shedding in all three cell lines.

3.5. The g345 siRNAs inhibit viral replication and $\gamma_1$34.5 expression in MG cells

To determine whether the g345 siRNAs inhibit $\gamma_1$34.5 and consequently the replication of the virus, $\gamma_1$34.5 and α-TIF gene expression was quantified using q-RT-PCR.

The gene α-TIF codes a virion transactivator protein and has previously been reported to reflect viral replication (Broberg et al., 2003). The expression of α-TIF is reduced in all cells treated with the known antiviral control UL29.2, and also in MG and HCE cells treated with the cytotoxic control 88bp, which causes apoptosis and thus effectively inhibits replication. This inhibited replication is also reflected in reduced $\gamma_1$34.5 expression, as inhibited replication reduces all viral gene expression.

The results of this study showed that g345 siRNAs significantly reduced $\gamma_1$34.5 expression in MG cells at 10 pmol/well (**Figure 8B**). The g345 siRNAs also reduced $\gamma_1$34.5 expression in MG cells at 1 pmol/well. However, this result is not statistically significant, as the g345-m treated sample has only a 3% expression compared to the infection only samples. This is due to large variation of the expression in the infection only samples.

The successful inhibition of $\gamma_1$34.5, a neurovirulence gene, in MG cells, that represent neuronal tissue, is reflected in the replication of the virus and as a result the α-TIF gene expression in the samples. All g345 treated samples at 10 pmol/well had significantly reduced expression, except for g345-cdt, which was slightly above p=0.05 (**Figure 8A**). Of the 1 pmol/well treated samples, only g345-fdt and g345-m showed a significant reduction in the α-TIF gene expression.

These results indicate that the g345 siRNAs successfully inhibit $\gamma_1$34.5 expression in MG cells that represent neuronal tissue and consequently reduce viral replication.

3.6. The g345 siRNAs induce varying innate immunity profiles in MG cells

To assess whether the g345 siRNA affect the innate responses in cells, ISG54, IFN-β, and IL-29 gene expressions were quantified. As $\gamma_1$34.5 inhibits interferon signaling, it was important to assess whether inhibiting the gene using RNA interference would affect the innate responses of the cells. As Vero cells lack interferon signaling, their innate responses were not quantified.

Cells treated with the cytotoxic control 88bp had increased ISG54, IFN-β, and IL-29 gene expression (**Figure 9**). The rest of the siRNA treated samples had much more inconsistent results. In HCE cells there are barely any significant differences to infection only in all of the gene expressions. However, in MG cells, an interesting trend regarding g345-c and g345-cdt is observable, which is an inhibited expression of all genes. Interestingly, samples treated with 10 pmol/well of g345-c lack IFN-β expression altogether, while g345-c and g345-cdt treated cells lack IL-29 expression and exhibit significantly decreased ISG54 expression. This reflects the viral shedding of the samples being increased. The IL-29 expression in MG cells is quite infrequent, where many samples lacked an IL-29 expression. This is perplexing as HCE cells seem unaffected.

3.7. The phenotype of the wild type virus resembles the vector backbone in MG cells treated with g345-f and g345-m

It is evident from the results that targeting nonessential genes of HSV-1 does not have an antiviral profile compared to that of UL29.2, which targets an essential gene. In all experiments, UL29.2 had reduced viral shedding and inhibited viral replication more efficiently and consistently than any g345 siRNA. However, one of the aims of this study was to observe whether $\gamma_1$34.5 RNA interference would change the phenotype of a wild type-like virus to that of a $\gamma_1$34.5 deletion vector. When comparing samples treated with 10 pmol/well of siRNA from the antiviral experiment in MG cells with untreated infected samples with the viral growth experiment in MG cells, a lot of commonalities can be observed. Although comparing the viral growth experiment results with the antiviral results (**Figure 5A** with **Figure 6**) is challenging as the cell confluency during time of infection was different (60% and 100% respectively), similarities in the reduction of GFP expression in cells infected with H1052 and infected LoxGFP cells treated with g345-f and g345-m are noticeable. At day 3 in the viral growth experiment, LoxGFP has a CPE of 100% in MG cells while H1052 has 25%. Although CPE is difficult to determine in the antiviral study, this trend seems to follow comparing untreated infected samples

(infection only) or infected samples treated with nonspecific siRNA (GL3) with infected cells treated with g345-f or g345-m. The reduction of viral shedding in g345 siRNA treated samples is tenfold, while the reduction of H1052 viral shedding compared to LoxGFP in the growth study was a hundredfold (**Figures 7A** and **5C**). In addition to the g345 siRNA failing to inhibit $\gamma_1$34.5 expression completely, differences in cell confluency can affect these results. Although these results indicate that $\gamma_1$34.5 RNA interference in wild type-like viruses changes the phenotype to resemble $\gamma_1$34.5 deletion vectors, repeated experiments with improved design would be required to confirm it.

3.8 The g345-c and -cdt siRNA-induced increase in viral shedding might be due to nonspecificity

Cells treated with g345-c and g345-cdt showed different responses in viral shedding and innate responses to that of cells treated with g345-f and g345-m. However, the q-RT-PCR results indicate that the inhibition of $\gamma_1$34.5 as well as the inhibition of replication was successful, yet the viral shedding was increased. Reflecting this increase in viral shedding is stunted innate immunity responses. Although the causal relationship of the decreased innate response in MG cells treated with g345-c and g345-cdt and an increase in viral titer is unclear, the decreased expression of α-TIF indicates that the increase in viral shedding is due to a compromised innate response, as opposed to a compromised innate response due to an increase in viral replication. This suggests that g345-c and g345-cdt are nonspecific and hit an unwanted target in MG cells.

3.9. The g345 siRNA lack an antiviral profile in HCE and Vero cells

Both the results of the viral shedding and the q-RT-PCR analyses indicate that the g345 siRNAs failed to inhibit $\gamma_1$34.5 in the HCE and Vero cells. While UL29.2 treatment in both HCE and Vero cells and 88bp treatment in HCE cells showed a significant decrease in viral shedding, the g345 siRNAs seemed more inconsistent in their antiviral profile (**Figures 7B** and **7C**). In HCE cells, only g345-m at 1 pmol/well had a significant decrease in viral shedding. In Vero cells, 10 pmol/well of g345-fdt and g345-m, as well as 1 pmol/well of g345-f, showed a significant decrease. However, in the 1 pmol/well plate GL3 also decreased viral shedding significantly, although the siRNA is nonspecific.

Furthermore, the quantification of gene expression shows that g345-mdt at 10 pmol/well in HCE cells had an increased $\gamma_1$34.5 expression, and cells treated with other g345 siRNA had no decreased expression (**Figure 8D**). Furthermore, α-TIF expression is unaffected

(**Figure 8C**). All innate responses fail to show a similar profile as MG cells with g345-c and g345-cdt, and the varying degrees of expression might be more arbitrary (**Figure 9**). The g345 siRNAs also fail to inhibit the expression of $\gamma_1$34.5, except for cells treated with 1 pmol/well of g345-fdt or GL3 (**Figure 8D**). 10 pmol of g345-fdt shows a significant reduction in α-TIF expression, but no other g345-siRNA reflects this result.

These results indicate that the $\gamma_1$34.5 inhibition was unsuccessful in both HCE and Vero cells, and whatever apparent antiviral efficacy can be observed is more likely due to other factors. This prompts the question why the g345 siRNAs successfully inhibit $\gamma_1$34.5 in MG cells but not in Vero cells.

There might have been a successful inhibition of $\gamma_1$34.5 in Vero cells, as $\gamma_1$34.5 deleted vectors are still able to replicate normally in them. Thus, $\gamma_1$34.5 inhibition would not be reflected in viral shedding or α-TIF expression. It may be that $\gamma_1$34.5 q-RT-PCR of cDNA synthesized with random hexamers could quantitate LAT, which is parallel to $\gamma_1$34.5 (**Figure 2**). This could be studied on existing samples by synthesizing cDNA using oligo-dT primers, and performing LAT q-RT-PCR.

However, it seems unlikely that $\gamma_1$34.5 inhibition was successful in HCE even if the q-RT-PCR quantitated LAT. As proven in the viral growth study, the growth of H1052 is reduced in HCE cells compared to LoxGFP (**Figure 5C**), indicating that an inhibition of $\gamma_1$34.5 should be reflected in reduced viral shedding or α-TIF expression. The difference in the g345 siRNAs' efficacy in different cell lines could be due to HCE being less transfectable than MG cells, as **Figure 4** suggests. However, UL29.2 still had as similar an antiviral efficacy in HCE cells as in MG cells, which indicates that the lack of antiviral efficacy in HCE cells is not only explained by lower transfectability.

Instead, the synthesis process of the siRNAs could affect how they are processed in different cells. Dicer sliced siRNAs are able to utilize any of the Argonaute proteins, whereas Argonaute 2 sliced siRNAs utilize Argonaute 2 exclusively (Sun et al., 2015, 2018). Literature regarding the upregulation or deregulation of Argonaute 2 in cancerous cells has been published extensively in the last decade (Cheng et al. 2013; Völler et al. 2013). These studies show that both upregulation and deregulation can be observed in different cancer cells, and suggest that there might be different expression of Argonaute 2 in HCE and MG cells, although HCE cells are immortalized while MG cells are of tumorous origin (refer to Materials and methods section 4.2). In this case, these differences could explain not only the differences in efficacy between the cell lines but also among the siRNAs.

3.10. The g345 siRNAs have a similar antiviral profile to that of cells treated with nonspecific siRNA against H1052

To assess whether the g345 siRNAs were specific to $\gamma_1$34.5, their efficacy was tested on the $\gamma_1$34.5 deleted vector H1052, which lacks the target of the siRNAs. It was hypothesized that these siRNAs would have a similar profile to that of nonspecific siRNAs like Sic-001, -003, and PET. The antiviral experiment was performed on MG cells, as they produced the best results when testing antiviral efficacy against the wild type-like virus LoxGFP. The experiment was performed identically to the experiments using LoxGFP.

The results show that UL29.2 has inhibited viral shedding of H1052 to the supernatant completely. The g345 siRNAs have a similar profile to that of Sic-001 and mock (lipofectamine only) treated samples, indicating that they are no more antiviral than nonspecific treatments. Most treatments show a reduced viral shedding compared to infection only samples, suggesting that the cellular responses to lipofectamine might also have antiviral efficacy on the viral shedding of H1052.

It can also be noted that 10 pmol/well of g345-cdt shows a significant increase in viral shedding, reflecting the results of LoxGFP, further suggesting that this siRNA is nonspecific.

However, quantifying H1052 was challenging, as its growth is slow compared to loxGFP, which might explain the variation of the treatments on different plates. For better results, repeated improved experiments are required.

3.11. Conclusions and future aspects

The results of this study show that $\gamma_1$34.5 RNA interference was successful in MG cells infected with wild type-like virus, and that the siRNA treatment are well tolerated. This inhibition also reduced viral replication as well as reduced viral shedding in samples treated with g345-f and g345-m, which makes these siRNAs promising for future studies. However, g345-c and g345-cdt seem to hit an unwanted target in the host genome, as viral shedding is increased even when $\gamma_1$34.5 and viral replication is reduced. These increases in viral shedding are reflected in a suppressed host response, although the causality of the relationship is uncertain.

The siRNAs g345-f and g345-m show antiviral efficacy in MG cells, although not to the extent of UL29.2. The phenotype of the wild type-like virus resembles that of H1052, although further studies are needed to confirm it. The results also indicate that the siRNAs

are not more antiviral than nonspecific siRNA against H1052, and furthermore, it seems that lipofectamine has antiviral qualities against H1052. Further studies of the innate responses on the samples could provide more information.

The $\gamma_1$34.5 inhibition was unsuccessful in Vero and HCE cells. The reason for this remains unclear. The $\gamma_1$34.5 q-RT-PCR could possibly quantitate LAT, and additional LAT q-RT-PCR analysis is needed. LAT q-RT-PCR would also be needed to confirm whether dTdT modifications affect the choice of target strand. The images of HCE cells transfected with Sic-003 also show that they might have lower transfectability than MG cells. Another possibility is their respective Argonaute protein family expressions differ, favoring differently synthesized siRNA. The quantitation of Argonaute expressions in these cell lines could provide information as to whether this hypothesis is plausible.

The results however are promising and g345-f and g345-m could be further studied for development of new infection models, as they showed antiviral efficacy and cellular tolerability on cells representing neurons. Furthermore, g345-f and g345-m could be used to design new selection methods, although determining why they have no antiviral profile in Vero and HCE cells would be required for this new method, unless the method is developed in MG cells.

4. Materials and Methods

4.1. siRNAs

Six siRNAs targeting $\gamma_1$34.5 were used in this study. Three different sequences were targeted, each having counterparts with dTdT modification at the 3' end (see **Table 1**.) Two of the sequences targeted by the siRNA are within the deleted region in HSV vectors while one is outside, common in HSV wild type and parental viruses (see **Figure 11**). The sequences of the siRNAs were chosen based on the maximal homology between the published sequences of Finnish HSV-1 strains (Bowen et al., 2019) and the reference strain HSV-1(17+) (J. Palomäki, unpublished). The siRNAs targeting $\gamma_1$34.5 are manufactured by Dharmacon (Lafayette, CO, USA).

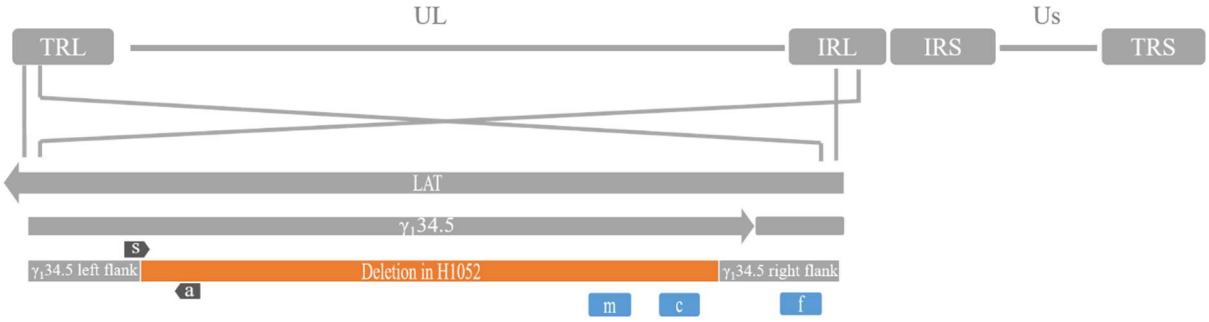

Figure 11. The relative location of the neurovirulence gene $\gamma_1$34.5. The location of $\gamma_1$34.5 in the HSV reference genome strain HSV-1(17+) is illustrated as well as the targets and locations of siRNAs (blue) and primers (black) (s = sense, a = antisense). The location of the deletion is illustrated in orange.

The controls of the siRNA treatment were the following: 88 base pair (bp) double stranded RNA as a positive toxic control, proven cytotoxic by Jiang et al. (2011), synthesized by our collaborative research group (dos. Minna Poranen group, Molecular and Integrative Biosciences Research Programme, University of Helsinki), using methods described previously by Romanovskaya et al. (2012); GFP-22, targeting eGFP as a nonspecific control, as used previously by Nygårdas et al (2009); UL29.2, targeting the UL29 gene of HSV-2 (Palliser et al., 2006) and of HSV-1 (Romanovskaya et al. 2012); Luciferase GL3 duplex targeting firefly luciferase coded by pGL3 reporter plasmid as a nonspecific control (Elbashir et al., 2001), manufactured by Dharmacon; a nonspecific control siRNA swarm targeting bacterial lac repressor sequences, as a nonspecific control, synthesized by Minna Poranen group; and commercial siRNAs (Sic 001 and

fluorescent Sic 003) as universal negative controls, manufactured by Sigma Aldrich (Saint Louis, MO, USA).

Table 1. RNAs used in this study.

siRNA	*length (bp)*	*type*	*target sequence*	*modification*	*reference*
g345-m	19	single site siRNA	HSV $\gamma_1$34.5 gene (1135-1153, 125221-125239)	none	Palomäki J. unpublished
g345-mdt	21		HSV $\gamma_1$34.5 gene (1135-1153, 125221-125239)	dTdT	
g345-c	18		HSV $\gamma_1$34.5 gene (1180-1197, 125177-125195)	none	
g345-cdt	20		HSV $\gamma_1$34.5 gene (1180-1977, 125177-125195)	dTdT	
g345-f	19		HSV $\gamma_1$34.5 gene flank (1312-1330, 125044-125062)	none	
g345-fdt	21		HSV $\gamma_1$34.5 gene flank (1312-1330, 125044-125062)	dTdT	
UL29.2	19		HSV-2 U_L29 gene (59931-59949)	none	Palliser et al., 2006
GFP-22	22		eGFP gene 22 nucleotide sequence		Nygårdas et al., 2009
GL3	21		Firefly luciferase gene (GL3 reporter plasmid)		Elbashir et al., 2001
Sic 001			Universal negative control		
Sic 003			Fluorescent universal negative control	Cyanine 3	
PET	401	siRNA swarm	bacterial lac-repressor, (nt 1630-2030 of pET32b vector)	none	Levanova et al., 2020
88bp	88	double stranded RNA	bacteriophage φ6 S segment, 88 nucleotide sequence		Jiang et al., 2011

4.2. Cells

For this research work HSV-susceptible human cell lines representing different tissues of origin were used. Vero cells (non-human primate kidney) were further used for production of viral stock and titration. The cell lines used included U251, a human glioblastoma cell line, here referred to as U373MG, originally obtained from ATCC (Manassas, VA, USA), which represents nervous system tissue. The cells were maintained in Dulbecco's modified eagle medium with Hepes (DMEM) (Gibco, Carlsbad, CA, USA) with 7% heat inactivated fetal bovine serum (FBS) (Serana, Silicon Valley, CA, USA), 2 mM glutaMAX (Gibco) and 200 µl/L gentamycin at 37°C in 5% CO_2. Also used was an African green monkey kidney cell line referred to as Vero cells (ATCC CCL-81), maintained in M199 (Biosera, Nuaille, France), 5% heat inactivated FBS, 2 mM glutaMAX and 200 µl/L gentamycin in 37°C 5% CO_2. The immortalized human corneal epithelial (HCE) cell line provided by prof. Arto Urtti (University of Helsinki, University of Kuopio), represents epithelial cells and was used for modeling corneal HSV infection. It was maintained in DMEM with Hepes, 7% heat inactivated FBS, 2 mM glutaMAX and 200 µl/L gentamycin in 37°C 5% CO_2.

The cells were divided weekly, detached using 10% Trypsin (Gibco) in phosphate buffered saline (PBS) HyClone (GE Healthcare Lifesciences, Marlborough, MA, USA) and counted using a cell counting kit (Bio-Rad, Hercules, CA, USA) and TC20 automated cell counter (Bio-Rad). The cells were cultured in T75 and T175 flasks (Sarstedt AG & Co. KG, Nümbrecht, Germany) and used for experiments in 96-well plates (Corning, Corning, NY, USA) for experiments.

4.3. Viruses

Two viral strains were used in this study. The first, a recombinant HSV-1 viral strain expressing a green fluorescent protein (GFP), HSV-1(17+) $LoxP_{mCMV}GFP$, abbreviated loxGFP, modified with methods described by Mattila et al. (2015), was obtained from Beate Sodeik (MHH Hannover Medical School). The second was a recombinant HSV-1 strain H1052 harboring a $\gamma_1$34.5 deletion and a pCMV-eGFP insert in the region, and with a luciferase insert between the genes UL55 and UL56 (Mattila et al. 2015). All viral strains were propagated in Vero cells and stored in MNT-buffer (20 nM Mes (Sigma Aldrich), 100 mM sodium chloride, 30 nM Tris (Bio-Rad)), as described previously by Romanavskaya et al. (2012).

The eGFP is expressed from the virus in infected cells from the mouse cytomegalovirus promoter after the alpha regulatory phase of HSV. The *in vitro* imaging was performed using an EVOS Auto FL live fluorescence microscope (Thermo Fisher Scientific, Waltham, MA, USA) using GFP filters for H1052 and LoxGFP infections.

4.4. Transfection

All cells were plated with antibiotic-free media prior to transfection. The cells were transfected when 60-70% confluent using the transfection reagent Lipofectamine RNAiMAX (Invitrogen, Carlsbad, CA, USA) according to the manufacturer's protocol and as previously described by Romanavskaya et al. (2012), with a modification of using a total volume of 100 µl per well. The cells were transfected with 1 or 10 pmol of the respective siRNA per well. Cells treated with transfection reagent only, mock transfections, were also included, as well as untreated cells, cells only controls. The treatments had five parallels.

The cells were washed and plated with 80 µl Opti-MEM (Gibco). The siRNA solution was combined with an Opti-MEM and Lipofectamine (97:3) solution in a 1:1 ratio and left to incubate for 20 minutes. 20 µl of the lipofectamine-siRNA complex was then pipetted to the corresponding well. The plates were put briefly on a shaker and then incubated in +37°C 5% CO_2 for 4 hours. Thereafter the cells were washed with DMEM 7% FBS, and maintained at +37°C 5% CO_2 with 200 µl of medium.

4.5. Infection

The cells were washed prior to the infection with DMEM with Hepes, 2% FBS and gentamycin. The viral MNT stock (stored in -80°C) was thawed on ice slowly. The cells (60-70% or 100% confluent) were infected with different amounts of plaque forming units depending on the experimental setting. In the antiviral assays, 1 000 pfu per well (equivalent to 0.1 MOI) was used, while in the viral growth monitoring setting, the cells were infected with five different amounts of virus (10 000, 1 000, 100, 10 and 1 pfu per well, equivalent to 0.7, 0.07, 0.007, 0.0007 and 0.00007 multiplicity of infection (MOI)). The dilution for infecting was made in DMEM with Hepes, 2% FBS, and gentamycin. After pipetting the dilution, the plates were put on a slow shaker for 1-2 hours at +35°C. Depending on the experiment, the cells were washed afterwards with DMEM 7% FBS and gentamycin, and 200 µl of upkeep medium added.

4.6. Viral production

Viruses were produced in Vero cells in cell master cell culture bottles (Greiner Bio-One, Kremsmünster, Austria) in DMEM 2% FBS with HEPES and gentamycin. The cells were infected at 70% confluency. Cells were harvested when they were 95% rounded and 80% detached. The cells were washed with PBS. The cell suspension was centrifuged for 5 minutes at 800 g and +4°C and the supernatant collected. The supernatant was centrifuged with a Beckman AVANTI J26 XP JA-14 rotor at 22 100 (max) g for 1h 45min at +4°C. The supernatant was discarded, and sterile filtered MNT buffer added to re-suspend the pellet overnight. The following day the viral stock was resuspended, aliquoted and stored in -80°C.

4.7. Cell viability assay

To ensure that the siRNAs were nontoxic to cells, cell viability assays of the siRNA treatments were performed. All siRNAs were tested using 1 and 10 pmol amounts per approximately 9000 cells. The assays were conducted 48 hours post transfection with CellTiter-Glo (Promega, Madison, WI, USA) luminescent assay, using the manufacturer's protocol and as described previously by Romanavskaya et al. (2012). The luminescense was quantified with VICTOR Nivo Multimode Plate Reader (Perkin Elmer, Waltham, MA, USA).

4.8. Antiviral assays

The antiviral efficacy was determined in a prophylactic model using methods previously described Romanovskaya et al. (2012). U373MG, HCE, and Vero cells were used. The cells were transfected with 1 pmol or 10 pmol of lipofectamine-siRNA complexes 4 hours prior to infection, proven efficacious by Levanova et al. (2020), with the methods described in section 4.4, at 60-70% confluency of the cells. The cells were then infected with 1 000 pfu/well of LoxGFP or H1052, with methods described in section 4.5.

Two days after infection the supernatant was collected to a parallel plate and stored at -80°C and the cells covered with 80 µl of TRI Reagent (Invitrogen) for RNA extraction and stored at -80°C.

4.9. Plaque titration

The viral titers were determined by titering the supernatant on Vero cells with a 100% confluency, with a 10-fold dilution series as previously described by Romanavskaya et al. (2012). The medium on the cells was changed to 100 µl DMEM with Hepes, 2% FBS and gentamycin. The plates with the supernatant was thawed slowly on ice. The supernatant was mixed thoroughly by pipetting, and the sample was transferred to the titration plate. After each dilution, the supernatant was mixed, and the pipet tips changed. After the infection, the plates were put on a shaker for 1-1.5h at +35°C. After incubation, 100 µl DMEM with Hepes, 7% FBS, gentamycin and 80 µl/L human immunoglobulin G (IgG) KIOVIG (Baxalta, Wien, Austria) was added to each well. Using medium containing IgG, viruses can only spread cell-to-cell, forming primary plaques.

After 3 days, the cells were fixed with methanol for 2-5 minutes, thereafter the methanol was removed and the wells were left to dry. After drying, 0.1% crystal violet (Merck kGaA, Darmstadt, Germany) diluted in PBS was added, and incubated at room temperature for 5 minutes. The crystal violet was removed, and the wells washed gently with tap water. After 1 day of drying at room temperature, the plaques were counted using light microscopy.

4.10. RNA extraction

The RNA extraction of the cell samples covered in TRI Reagent was performed according to the manufacturer's protocol. Chloroform (20% of TRI Reagent volume) was added to the sample, incubated and centrifuged. The aqueous phase was separated, and the RNA precipitated from it using isopropanol (50% of TRI Reagent volume), incubated and centrifuged. After the isopropanol was discarded, the pellet was re-suspended and precipitated in 70% ethanol and centrifuged. The ethanol was discarded, and the pellet dried on Savant SVC-100H SpeedVac concentrator (Thermo Fischer Scientific). The pellet was re-suspended in 20 µl of nuclease free water and stored at -80°C.

4.11. cDNA synthesis

The cellular RNA extracted from the cell samples was processed into complementary DNA (cDNA) using a reverse transcriptase (RT) reaction as previously described (Romanovskaya et al., 2012). The samples were treated with DNase (Thermo Fischer Scientific, Waltham, MA, USA) and RNase inhibitor (Thermo Fischer Scientific) for 30 minutes at 37°C using a MJ Research PTC-200 Peltier Thermal Cycler (Bio-Rad). The

DNase was then inhibited using EDTA (Thermo Fischer Scientific) at 65°C for 10 minutes. Random hexamer primers (Thermo Fischer Scientific) were annealed for 5 minutes at 70°C. RevertAid H Reverse Transcriptase (Thermo Fischer Scientific) and dNTPs (Thermo Fischer Scientific) were added and the RT cycle run as following: 20 minutes at 37°C, 60 minutes at 42°C, 10 minutes at 70°C and cooling down at 4°C. After the reaction, the cDNA was stored at -80°C.

4.12. Quantitative real-time PCR

Quantitative real-time PCR (q-RT-PCR) was performed on the synthesized cDNA samples using a Rotor-Gene Q instrument (Qiagen, Hilden, Germany). SYBR Green enzyme kit (Thermo Fischer Scientific) was utilized as previously described by Nygårdas et al (2011). The primers used are defined in **Table 2**, and the location of the primers for quantifying the $\gamma_1$34.5 mRNA expression are illustrated in **Figure 11**. Gene expression was quantified and normalized to each sample's respective GAPDH expression. The q-RT-PCR was done using corresponding quantification standards in a tenfold serial dilution from 10^8 to 10^1 copies/reaction. The standards are either larger PCR products, plasmids or isolated DNA (see to **Table 3** for the primers or templates used to create the standards).

Table 2. Primers for q-RT-PCR used in this study.

Target	Sequence (upper sense, lower antisense)	Annealing temperature	Reference
GAPDH	GAG AAG GCT GGG GCT CAT TGC TGA TGA TCT TGA GGC TG	55°C	Nygårdas et al., 2009
αTIF/VP16	GCT CCG TTG ACG AAC ATG AA TTT GAC CCG CGA GAT CCT AT	60°C	Broberg et al., 2003
$\gamma_1$34.5	ACA GTC CCA GGT AAC CTC CA AGC AGC AGC GAA CAA GAA G	60°C	This study
ISG54	ACT ATC ACA TGG GCC GAC TC TTT AAC CGT GTC CAC CCT TC	55°C	Romanovskaya et al., 2012
IFN-β	TCT CCA CGA CAG CTC TTT CCA ACA CTG ACA ATT GCT GCT TCT TTG	60°C	Peri et al., 2008
IL-29/IFN-λ1	GAC GCC TTG GAA GAG TCA C CTC ACC TGG AGA AGC CTC A TCC TCC GTA TCC TCG CTT TA	60°C	Paavilainen et al., 2015

Table 3. Primers or template used to create standard for q-RT-PCR used in this study.

Standard	Primers or template used to create standard (upper sense, lower antisense)
GAPDH	AAT CCC ATC ACC ATC TTC CA
	TGA GTC CTT CCA CGA TAC CA
αTIF/VP16	α-TIF plasmid pRB3717 (McKnight et al., 1987)
$\gamma_1$34.5	DNA isolated from HSV-1 strain 17+
ISG54	AAG CCA CAA TGT GCA ACC TA
	GAG CCT TCT CAA AGC ACA CC
IFN-β	AGA CTG CTC ATG CGT TTT CC
	TCC TCC AAA TTC CTC TCC TG
IL-29/IFN-λ1	GAC TTT GGT GCT AGG CTT GG
	AAG GTG ACA GAT GCC TCC AG

4.13. Statistical analysis

The normality of the data was assessed visually. The exact statistical significance was calculated with SPSS statistics 25 (IBM, Armonk, NY, USA) using Mann Whitney's non-parametric U-test comparing two individual groups.

Acknowledgements

I would like to thank Veijo Hukkanen and Marie Nyman as well as Kiira Kalke and Liisa Lund for being welcoming, patient and helpful. I have learned a lot during this past year.

I would also like to acknowledge Jussi Palomäki for designing the g345 siRNAs. Furthermore, I would like to acknowledge Beate Sodeik for providing LoxGFP, and prof. Arto Urtti for providing HCE cells.

The study was supported by the grant #170046 from the Jane and Aatos Erkko Foundation.

List of Abbreviations

CPE – cytopathic effect

ds – double stranded

GFP – green fluorescent protein

HSV – herpes simplex virus

ICP – infected cell protein

IFN – interferon

IL – interleukin

ISG – interferon stimulated gene factor

MOI – multiplicity of infection

pfu – plaque forming unit

siRNA – small interfering RNA

References

Andtbacka, R.H., H.L. Kaufman, F. Collichio, T. Amatruda, N. Senzer, J. Chesney, K.A. Delman, L.E. Spitler, I. Puzanov, S.S. Agarwala, M. Milhem, L. Carnmer, B. Curti, K. Lewis, M. Ross, T. Guthrie, G.P. Linette, G.A. Daniels, K. Harrington, M.R. Middleton, W.H. Miller Jr, J.S. Zager, Y. Ye, B. Yao, A. Li, S. Doleman, A. VanderWalde, J. Gansert, and R.S. Coffin. 2015. Talimogene Laherparepvec Improves Durable Response Rate in Patients with Advanced Melanoma. *J Clin Oncol*. 33(25):2780-2788. doi:10.1200/JCO.2014.58.3377

Broberg, E., M. Nygårdas, A.A. Salmi, and V. Hukkanen. 2003. Low copy number detection of herpes simplex virus type 1 mRNA and mouse Th1 type cytokine mRNAs by Light Cycler quantitative real-time PCR. *J Virol Methods*. 112:53-65.

Broberg, E., J. Peltoniemi, M. Nygårdas, T. Vahlberg, M. Röyttä, and V. Hukkanen. 2004. Spread and Replication of and Immune Response to 134.5-Negative Herpes Simplex Virus Type 1 Vectors in BALB/c Mice. *Journal of virology*. 78(23):13139– 13152. doi:10.1128/JVI.78.23.13139-13152.2004

Brown, Z.A., A. Wald, R.A. Morrow, S. Selke, J. Zeh, and L. Corey. 2003. Effect of serologic status and cesarean delivery on transmission rates of herpes simplex virus from mother to infant. *JAMA*. 289:203-209. doi:10.1001/jama.289.2.203

Bhuyan, P. K., K. Karikò, J. Capodici, J. Lubinski, L.M. Hook, H.M. Friedman, and D. Weissman. 2004. Short interfering RNA-mediated inhibition of herpes simplex virus type 1 gene expression and function during infection of human keratinocytes. *Journal of virology*. 78(19):10276–10281. doi:10.1128/JVI.78.19.10276-10281.2004

Cheng, N., Y.D. Li, and Z.G. Han. 2013. Argonaute2 Promotes Tumor Metastasis by Way of Up-regulating Focal Adhesion Kinase Expression in Hepatocellular Carcinoma. *Hepatology*. 57(5):1906-18. doi:10.1002/hep.26202

Connolly, S. A., J.O. Jackson, T.S. Jardetzky, and R. Longnecker. 2011. Fusing structure and function: a structural view of the herpesvirus entry machinery. *Nature reviews. Microbiology*. *9*(5): 369–381. doi:10.1038/nrmicro2548

Denes, C.E., R.D. Everett, and J. Russell. 2020. Diefenbach. Tour de Herpes: Cycling Through the Life and Biology of HSV-1. In Herpes simplex virus: Methods and protocols.

Diefenbach, R.J., C. Fraefel, editors. Methods in molecular biology. 2 nd ed. 1-26.

Goins W.F., S. Huang, B. Hall, M. Marzulli, J.B. Cohen, and J.C. Glorioso. 2020. Engineering HSV-1 Vectors for Gene Therapy. In Herpes simplex virus: Methods and protocols.

Diefenbach, R.J., C. Fraefel, editors. Methods in molecular biology. 2 nd ed. 73-88.

Hukkanen V., H. Paavilainen, and R. Mattila. 2010. Host responses to herpes simplex virus and herpes simplex virus vectors. *Future virology*. 5(4):493-512. doi:10.2217/fvl.10.35

Elbashir, S.M., J. Harborth, W. Lendeckel, A. Yalcin, K. Weber, and T. Tuschl. 2001. Duplexes of 21-nucleotide RNAs mediate RNA interference in cultured mammalian cells. *Nature*. 411(6836):494-8. doi: 10.1038/35078107

Farooq, A.V., D. Shukla. 2012. Herpes simplex epithelial and stromal keratitis: an epidemiologic update. *Surv Ophthalmol*. 7(5):448-62. doi:10.1016/j.survophthal.2012.01.005

Falko, S., and J.P. Weir. 2007. Incorporation of a lambda phage recombination system and EGFP detection to simplify mutagenesis of Herpes simplex virus bacterial artificial chromosomes. *BMC biotechnology*. 7(22). doi:10.1186/1472-6750-7-22

Fire, A., S.Q. Xu, M.K. Montgomery, S.A. Kostas, S.E. Driver, and C.C Mello. 1998. Potent and specific genetic interference by double-stranded RNA in *Caenorhabditis elegans*. *Nature.* 391**:**806–811. https://doi.org/10.1038/35888

Grünwald, K., P. Desai, D.C. Winkler, J.B. Heymann, D.M. Belnap, W. Baumeister, and A.C. Stevens. 2003. Three-dimensional structure of herpes simplex virus from cryo-electron tomography. *Science*. 302:1396-1398. doi:10.1126/science.1090284

Honess, R.W., and B. Roizman. 1974. Regulation of herpesvirus macromolecular synthesis. I. Cascade regulation of the synthesis of three groups of viral proteins. *J Virol*. 14(1):8-19. doi:10.1128/JVI.14.1.8-19.1974

Hukkanen, V., and M. Seppänen. 2020. Herpes simplexvirukset. In Mikrobiologia. Duodecim. Retrieved 28.08.20 from https://www.oppiportti.fi/op/mbg00406/do

Hukkanen, V., and P.Vihinen. 2016. Onkolyyttinen geenihoitovirus tulossa osaksi ihomelanooman lääkehoitoa. Suom Lääk äril; 71: 818–820. Retrieved 28.08.20 from https://www.laakarilehti.fi/tyossa/laakeinfo/onkolyyttinen-geenihoitovirus-tulossaosaksi-ihomelanooman-laakehoitoa/

Hwang, J., C. Chang, J.H. Kim, C.T. Oh, H.N. Lee, C. Lee, D. Oh, C. Lee, B. Kim, S.W. Hong, and D.K. Lee. 2016. Development of Cell-Penetrating Asymmetric Interfering RNA Targeting Connective Tissue Growth Factor. *Journal of Investigative Dermatology*. 136(11):2305-2313. doi:10.1016/j.jid.2016.06.626

Javanbakht, H, H. Mueller, J. Walther, X. Zhou, A. Lopez, T. Pattupara, J. Blaising, L. Pedersen, N. Albæk, M. Jackerott, T. Shi, C. Ploix, W. Driessen, R. Persson, J. Ravn, J. Young, and S. Ottosen. 2018. Liver-Targeted Anti-HBV Single-Stranded Oligonucleotides with Locked Nucleic Acid Potently Reduce HBV Gene Expression In Vivo. *Molecular Therapy - Nucleic Acids.* 11:441-454. doi: 10.1016/j.omtn.2018.02.005

Jiang, M., P. Osterlund, L.P. Sarin, M.M. Poranen, D.H. Bamford, D. Guo, and I. Julkunen. 2011. Innate immune responses in human monocyte-derived dendritic cells are highly dependent on the size and the 5' phosphorylation of RNA molecules. *J Immunol*. 187 (4):1713-1721. doi:10.4049/jimmunol.1100361

Jin, F., S. Li, K. Zheng, C. Zhuo, K. Ma, M. Chen, Q. Wang, P. Zhang, J. Fan, Z. Ren, and Y. Wang. 2014. Silencing herpes simplex virus type 1 capsid protein encoding genes by siRNA: a promising antiviral therapeutic approach. *PloS one*. 9(5), e96623. doi:10.1371/journal.pone.0096623

Kalke, K., J. Lehtinen, J. Gnjatovic, L.M. Lund, M.C. Nyman, H. Paavilainen, J. Orpana, T. Lasanen, F. Frejborg, A.A. Levanova, T. Vuorinen, M.M. Poranen, and V. Hukkanen. 2020. Herpes Simplex Virus Type 1 Clinical Isolates Respond to UL29-Targeted siRNA Swarm Treatment Independent of Their Acyclovir Sensitivity. *Viruses*. 12(12):1434. doi: 10.3390/v12121434

Kim, J.Y., A. Mandarino, M.V. Chao, I. Mohr, and A.C. Wilson. 2012. Transient reversal of episome silencing precedes VP16-dependent transcription during

reactivation of latent HSV-1 in neurons. *PLoS Pathog*. 8(2):e1002540. doi:10.1371/journal.ppat.1002540.

Knipe, D., P. Howley, J. Cohen, D. Griffin, R. Lamb, M. Malcolm, V. Racanciello, and B. Roizman. 2013. Herpes simplex viruses. In Fields Virology. 6 th e. Wolters Kluwer health. 2:1824-1892.

Kumar, V., A. Abbas, and J Aster. 2013. Robbins basic pathology. Elsevier Inc. 827-828.

Levanova, A.A., K.M. Kalke, L.M. Lund, N. Sipari, M. Sadeghi, M. C. Nyman, H. Paavilainen, V. Hukkanen, and M.M. Poranen. 2020. Enzymatically synthesized 2′-fluoro-modified Dicer-substrate siRNA swarms against herpes simplex virus demonstrate enhanced antiviral efficacy and low cytotoxicity. *Antiviral research*. 182. doi:10.1016/j.antiviral.2020.104916

Linderman, J.A., M. Kobayashi, V. Rayannavar, J.J. Fak, R.B. Darnell, M.V. Chao, A.C. Wilson, and I. Mohr. 2017. Immune Escape via a Transient Gene Expression Program Enables Productive Replication of a Latent Pathogen. *Cell Reports*. 18(5):1312-1323. doi:10.1016/j.celrep.2017.01.017

Linehan, J.L., O.J Harrison, S.J. Han, A.L. Byrd, I. Vujkovic-Cvijin, A.V. Villarino, S.K. Sen, J. Shaik, M. Smelkinson, S. Tamoutounour, N. Collins, N. Bouladoux, A. Dzutsev, S.P. Rosshart, J.H. Arbuckle, C.R. Wang, T.M. Kristie, B. Rehermann, G. Trinchieri, J.M. Brenchley, and Y. Belkaid. 2018. Non-classical Immunity Controls Microbiota Impact on Skin Immunity and Tissue Repair. *Cell*, *172*(4), 784–796.e18. doi.org:10.1016/j.cell.2017.12.033

Liptak, L.M., S.L. Uprichard, and D.M. Knipe. 1996. Functional order of assembly of herpes simplex virus DNA replication proteins into prereplicative site structures. *J Virol*. 70(3):1759-67. doi:10.1128/JVI.70.3.1759-1767.1996

Loret, S., G. Guay, and R. Lippé. 2008. Comprehensive characterization of extracellular herpes simplex virus type 1 virions. *J Virol*. 82:8605-8618.

Lumio, J. 2020. Aivotulehdus (enkefaliitti, “aivokuume”). Lääkärikirja Duodecim. Retrieved 24.0.8.20 from https://www.terveyskirjasto.fi/terveyskirjasto/tk.koti?p_artikkeli=dlk00559

Mattila, R.K., K. Harila, S.M. Kangas, H. Paavilainen, A.M. Heape, I.J. Mohr, and V. Hukkanen. 2015. An investigation of herpes simplex virus type 1 latency in a novel mouse dorsal root ganglion model suggests a role for ICP34.5 in reactivation. *J Gen Virol*. 96(8):2304- 2313. doi:10.1099/vir.0.000138

McKnight, J.L., T.M. Kristie, and B. Roizman. 1987. Binding of the virion protein mediating alpha gene induction in herpes simplex virus 1-infected cells to its cis site requires cellular proteins. *Proc Natl Acad Sci U S A*. 84(20):7061- 7065

Meyding-Lamadé, U., W. Lamadé, R. Kehm, K.W. Knopf, T. Heß, G. Gosztonyi, O. Degen, W. Hacke. 1998. Herpes simplex virus encephalitis: cranial magnetic resonance imaging and neuropathology in a mouse model. Neuroscience Letters. 248(1):13-16. doi:.1016/S0304-3940(98)00319-X

Mettenleiter T.C. 2002. Herpesvirus assembly and egress. *J Virol*. 76(4):1537-47. doi:10.1128/jvi.76.4.1537-1547.2002

Myllys, M., V. Ruokolainen, V. Aho, E.A. Smith, S. Hakanen, P. Peri, A. Salvetti, J. Timonen, V. Hukkanen, C.A. Larabell, and M. Vihinen-Ranta. 2016. Herpes simplex virus 1 induces egress channels through marginalized host chromatin. *Sci Rep*. 6:28844. doi:10.1038/srep28844

Mäki, J., H. Paavilainen, S. Grénman, S. Syrjänen, and V. Hukkanen 2015. Carriage of herpes simplex virus and human papillomavirus in oral mucosa is rare in young women: A long-term prospective follow-up. *Journal of clinical virology*. 70:58-62. doi:10.1016/j.jcv.2015.07.006

Nygårdas, M., T. Vuorinen, A.P. Aalto, D.H. Bamford, and V. Hukkanen. 2009. Inhibition of coxsackievirus B3 and related enteroviruses by antiviral short interfering RNA pools produced using w6 RNA-dependent RNA polymerase. *Journal of general virology*. 90:2468– 2473. doi:10.1099/vir.0.011338-0

Paavilainen, H., A. Romanovskaya, M. Nygårdas, D.H. Bamford, M.M. Poranen, and V. Hukkanen. 2015. Innate responses to small interfering RNA pools inhibiting herpes simplex virus infection in astrocytoid and epithelial cells. *Innate Immun*. 21(4):349-57. doi: 10.1177/1753425914537921

Paavilainen, H., J. Lehtinen, A. Romanovskaya A, M. Nygårdas, D.H. Bamford, M.M. Poranen, and V. Hukkanen. 2016. Inhibition of clinical pathogenic herpes simplex virus 1 strains with enzymatically created siRNA pools. *J Med Virol*. 88(12):2196-2205. doi:10.1002/jmv.24578

Paavilainen, H., J. Lehtinen, A. Romanovskaya, M. Nygårdas, D.H. Bamford, M.M. Poranen, and V. Hukkanen. 2017. Topical treatment of herpes simplex virus infection with enzymatically created siRNA swarm. *Antivir Ther*. 22(7):631-637. doi: 10.3851/IMP3153

Palliser, C., D. Chowdhury, Q.Y. Wang, S.J. Lee, T. Bronson, D.M. Knipe, and J. Lieberman. 2006. An siRNA-based microbicide protects mice from lethal herpes simplex virus 2 infection. *Nature*. 439:89-94.

Peri, P., R.K. Mattila, H. Kantola, E. Broberg, H.S. Karttunen, M. Waris, T. Vuorinen, and V. Hukkanen. 2008. Herpes simplex virus type 1 Us3 gene deletion influences toll-like receptor responses in cultured monocytic cells. *Virol J*. 5:140.

Perng, G.C., and C. Jones. 2010. Towards an understanding of the herpes simplex virus type 1 latency-reactivation cycle. *Interdiscip Perspect Infect Dis*. 262415. doi:10.1155/2010/262415

Rand, T., S. Peterson, F.H. Du, and X.D. Wang. 2005. Argonaute2 cleaves the anti-guide strand of siRNA during RISC activation. *Cell*. 123(4):621-629 doi:10.1016/j.cell.2005.10.020

Roizman, B., and F. Jenkins. 1985. Genetic engineering of novel genomes of large DNA viruses. *Science*. 229:1208-1213.

Romanovskaya, A., H. Paavilainen, M. Nygårdas, D.H. Bamford, V. Hukkanen, and M.M. Poranen. 2012. Enzymatically produced pools of canonical and Dicer-substrate siRNA molecules display comparable gene silencing and antiviral activities against herpes simplex virus. *PloS One*. 7(11). doi:10.1371/journal.pone.0051019

Sandbaumhüter, M., K. Döhner, J. Schipke, A. Binz, A. Pohlmann, B. Sodeik, and R. Bauerfeind. 2013. Cytosolic herpes simplex virus capsids not only require binding inner tegument protein pUL36 but also pUL37 for active transport prior to secondary envelopment. *Cellular microbiology*. 15(2):248–269. doi:10.1111/cmi.12075

Silva, A.P., J.F. Lopes, and V.S. Paula. 2014. RNA interference inhibits herpes simplex virus type 1 isolated from saliva samples and mucocutaneous lesions. *Braz J Infect Dis*. 18(4):441-444. doi:10.1016/j.bjid.2014.01.011

Silva, A.S., J.V. Raposo, T.C. Pereira, M.A. Pinto, and V.S. Paula. 2016. Effects of RNA interference therapy against herpes simplex virus type 1 encephalitis. *Antivir Ther*. 21(3):225-235. doi:10.3851/IMP3016

Sodeik, B., M. Ebersold, and A. Helenius. (1997). Microtubule-mediated Transport of Incoming Herpes Simplex Virus 1 Capsids to the Nucleus. *The Journal of cell biology*. 136. 1007-21

Song, B., X. Liu, Q. Wang, R. Zhang, T. Yang, Z. Han, and Y. Xu. 2016. Adenovirus-mediated shRNA interference against HSV-1 replication *in vitro*. *J Neurovirol*. 22(6):799-807. doi:10.1007/s13365-016-0453-4

Stevens, J.G., E.K. Wagner, G.B. Devi-Rao, M.L. Cook, and L.T. Feldman. 1987. RNA complementary to a herpesvirus alpha gene mRNA is prominent in latently infected neurons. *Science*. 235:1056-1059. doi:10.1126/science.2434993

Sun, G., J.H Wang, Y.S. Huang, C.W.Y. Yuan, K.Q. Zhang, S.Y. Hu, L.L Chen, R.J. Lin, Y. Yen, and A.D. Riggs. 2018. Differences in silencing of mismatched targets by sliced versus diced siRNAs. *Nucleic Acids Research*. 46(13):6806–6822. doi:10.1093/nar/gky287

Sun, G., S.Y. Yeh, C.W. Yuan, M.J. Chiu, B.S. Yung, and Y. Yen. 2015. Molecular Properties, Functional Mechanisms, and Applications of Sliced siRNA. *Molecular therapy. Nucleic acids*. 4(1). e221. doi:10.1038/mtna.2014.73

Völler, D., J. Reinders, G. Meister, and A.K. Bosserhoff. 2013. Strong reduction of AGO2 expression in melanoma and cellular consequences. *British journal of cancer*. 109(12):3116–3124. doi:10.1038/bjc.2013.646

Whitley, R.J., E.R. Kern, S. Chatterjee, J. Chou, and B. Roizman. 1993. Replication, establishment of latency, and induced reactivation of herpes simplex virus gamma 1 34.5 deletion mutants in rodent models. *The Journal of clinical investigation*. 91(6):2837–2843. https://doi.org/10.1172/JCI116527

Zhang, Y.Q., W. Lai, H. Li, and G. Li. 2008. Inhibition of herpes simplex virus type 1 by small interfering RNA. *Clinical and experimental dermatology*. 33(1):56–61. doi:10.1111/j.1365-2230.2007.02543.x